Efficient Piecewise Trees for the Generalized Skew Vasicek Model with Discontinuous Drift

Xiaoyang Zhuo* **and Olivier Menoukeu-Pamen**[†,‡]

Abstract

In this paper, we explore two new tree lattice methods, the piecewise binomial tree and the piecewise trinomial tree for both the bond prices and European/American bond option prices assuming that the short rate is given by a generalized skew Vasicek model with discontinuous drift coefficient. These methods build nonuniform jump size piecewise binomial/trinomial tree based on a tractable piecewise process, which is derived from the original process according to a transform. Numerical experiments of bonds and European/American bond options show that our approaches are efficient as well as reveal several price features of our model.

Keywords: Skew Vasicek model; discontinuous drift; binomial tree; trinomial tree.

1. Introduction

The application of skew diffusions in modeling asset prices and interest rates has been widely used in the recent years due to their special path features. For example, such models enable to take into account long duration of asset prices (Zhuo *et al.*, 2016a), or prices in a target zone (Xu *et al.*, 2016). The objective of this paper is two-fold: First, it aims at modeling short rate with the skew Vasicek model with discontinuous drift coefficient. Second, it introduces new piecewise binomial and trinomial lattice approaches to solve both bond and European/American bond option pricing under this model.

The classical skew Vasicek model is a particular type of skew diffusion model which is an extension of the skew Brownian motion introduced by Itô & McKean (1965). The latter can be seen as a sign reversing of excursions of standard Brownian motion with a certain probability p and has been

*Department of Financial Management, Business School, Nankai University, Tianjin, 300071, P.R.China. Email: zhuoxy3600@mail.nankai.edu.cn.
†African Institute for Mathematical Sciences, University of Ghana, Ghana; Institute for Financial and Actuarial Mathematics, University of Liverpool, Liverpool, L69 7ZL, United Kingdom. Email: Menoukeu@liv.ac.uk.
‡Corresponding author.

studied extensively in the literature, see, for example, Walsh (1978); Harrison & Shepp (1981); Le Gall (1984); Ouknine (1990); Ouknine & Rutkowski (1995); Barlow *et al.* (2000); Appuhamillage & Sheldon (2012). This process is reduced to the standard Brownian motion when $p = 0.5$ and is equal to the reflected Brownian motion when $p \in \{0, 1\}$.

As for applications of this model to physics, biology, geophysics and astrophysics, the reader may consult Lang (1995), Cantrell & Cosner (1999), Lejay (2003) and Zhang (2000), respectively. We also refer to Decamps *et al.* (2004, 2005, 2006a,b); Corns & Satchell (2007); Rossello (2012); Gairat & Shcherbakov (2016) for some interesting applications in finance. In equity derivative pricing, the paper Decamps *et al.* (2004) studies European options on a diffusion with discontinuous volatility using a skew functional integral, whereas the work Decamps *et al.* (2006a) derives the Laplace transform of perpetuities and weighted Asian option based on asymmetric skew Bessel process. Let us also mention the interesting work Gairat & Shcherbakov (2016), where the authors derive the joint distribution of skew Brownian motion and some of its functionals, and use these results to price European option under both a discontinuous local volatility model and a displaced diffusion model with constrained volatility.

Recently, the skew Vasicek (or skew Ornstein-Uhlenbeck) process has been introduced to model interest rates and asset prices. This model has the advantage that it has both features of a skew process and an Ornstein-Uhlenbeck process. Wang *et al.* (2015) prove the existence and uniqueness of the solution of the stochastic differential equation satisfied by the skew Ornstein-Uhlenbeck process. Then they price a zero-recovery defaultable bond and the conditional default probability with incomplete information assuming that the asset follows a skew Ornstein-Uhlenbeck process. Song *et al.* (2015) give the explicit Laplace transforms for the first hitting times of doubly skewed Ornstein-Uhlenbeck process by means of Hermite functions.

In this paper, we extend the skew Vasicek model to the case of discontinuous drift coefficient. In particular, we assume that the drift has a two state-dependent long-term mean. The reasons for applying this generalized model to interest rate market are due to: First, the mean reversion property of the Vasicek model can capture the dynamics of interest rates which tend to revert to the long-term mean because of macroeconomic arguments. Second, interest rates staying at some specific levels for a prolonged period of time can be frequently observed, such as the popular long-lasting near-zero interest rate in U.S., Japan, Switzerland, etc. Such a phenomenon is referred to as the *long duration* of interest rates (Zhuo *et al.*, 2016a). The skew processes, which can force the dynamics of interest rates or asset prices to stay below/above some levels with high/small probability, are

suitable for reproducing this long duration phenomenon. For example, Zhuo *et al.* (2016a) use the skew constant-elasticity-of-variance (CEV) model to replicate the interest rates hovering at some specific levels for a long-lasting period, due to its flexible manipulation of duration movements. Last, the regime switching features of interest rates are also common in reality (see e.g., Pfann *et al.* (1996); Decamps *et al.* (2006b)), thus it is simple and straightforward to introduce the state-dependent long-term mean scheme. In this way, our generalized model can capture different long-run tendencies in different states of the economy.

In the generalized skew Vasicek model with discontinuous drift, the closed-form solutions for prices of bonds, options, and other nonstandard derivatives cannot be obtained. In this case, we use numerical methods to compute derivative prices. First, we adopt a one-to-one transformation technique to obtain a tractable piecewise diffusion process without local time. This transform is similar to that in Zhuo *et al.* (2016a) and Zhuo *et al.* (2016b), who use a two-step transform to the skew CEV model and the skew CIR model, respectively. By doing so, it is possible to apply the useful tree lattice approach to the transformed process. However, the transformation is carried out at the expense of nonuniform piecewise volatilities, under which the classical tree construction is not feasible. In fact, to ensure that the tree recombines, the jump sizes in a tree, which are decided by the volatility, must be identical. But with piecewise nonuniform volatilities, there is no guarantee that the jump sizes are equal in the global region. To overcome this obstacle, we then propose a piecewise binomial tree similar to that in Zhuo *et al.* (2016a) for the generalized skew Vasicek model with discontinuous drift. The authors in the above work propose a piecewise binomial tree for the transformed skew CEV model in three situations of the volatility elasticity parameter. In each situation, the jump sizes are different for two subregions. In our modified binomial tree, the whole region is also divided into two subregions. Jump sizes are the same for respective subregions, such that the tree recombines in each subregion. But the jump sizes are different for different subregions, so as to match the different piecewise volatilities in the transformed process. In order to ensure the tree still recombines when jumping from one subregion to the other one, a special treatment for the boundary nodes between two subregions is put forward. Additionally, we also extend the piecewise binomial tree to the more accurate trinomial tree, which allows the nodes to move upwards, downwards, or stay at the same level in the next step. Finally, in our numerical experiments, we calculate zero-coupon bond prices and European/American bond option prices by using the proposed piecewise binomial and trinomial tree lattice approaches. Generally, the trinomial lattice performs better than the binomial one. The simulation results also reveal many interesting features of the

generalized Vasicek model with discontinuous drift, such as the patterns of the "skew effect" (price deviation from non-skew price), and the influence of discontinuous drift scheme on bond prices.

The rest of the paper is organized as follows: Section 2 defines the generalized skew Vasicek model with discontinuous drift, and provides the details of the transformation scheme to remove the local time. Based on the transformed process, Section 3 and Section 4 illustrate the detailed lattice construction steps of the piecewise binomial tree and the piecewise trinomial tree, respectively. Section 5 exhibits the results of simulation experiments to show the price patterns of bond, European and American bond options under the generalized skew Vasicek model with discontinuous drift. The conclusions are drawn in Section 6.

2. The Generalized Skew Vasicek Model with Discontinuous Drift

To begin with, fix the complete probability space $(\Omega, \mathcal{F}, Q)$ with the filtration $\{\mathcal{F}_t\}_{t\geq 0}$ satisfying the usual conditions. Q represents the risk-neutral measure. Assume the dynamics of short rate are governed by the following stochastic differential equation (SDE) with local time and discontinuous drift

$$\begin{aligned} \mathrm{d}r_t &= k\left(\theta_1 \mathbb{1}_{\{r_t<a_1\}} + \theta_2 \mathbb{1}_{\{r_t\geq a_1\}} - r_t\right)\mathrm{d}t + \sigma \mathrm{d}W_t + (2p-1)\,\mathrm{d}\hat{L}_t^r(a_2) \\ &= \begin{cases} k\left(\theta_1 - r_t\right)\mathrm{d}t + \sigma \mathrm{d}W_t + (2p-1)\,\mathrm{d}\hat{L}_t^r(a_2), & r_t < a_1, \\ k\left(\theta_2 - r_t\right)\mathrm{d}t + \sigma \mathrm{d}W_t + (2p-1)\,\mathrm{d}\hat{L}_t^r(a_2), & r_t \geq a_1, \end{cases} \end{aligned} \tag{1}$$

where W_t is a standard Brownian motion, $k > 0$ measures the speed of mean reversion, $\sigma > 0$ stands for the short rate volatility. θ_1 and θ_2 are state-dependent long-term means in low interest rate environment ($r_t < a_1$) and high interest rate environment ($r_t > a_1$), respectively. $\hat{L}_t^r(a_2)$ is the symmetric local time of the short rate process r_t at the *skew level* a_2. The *skew probability* $p \in (0,1)$ captures the upward probability when r_t hits the skew level a_2. That is, the paths of short rate behave like those without local time before and after hitting the skew level a_2. However, as long as the short rate touches the level a_2, it would produce an upward movement for r_t with probability p and a downward movement with corresponding probability $1-p$. Notably, when $p = 0.5$, the local time vanishes; when $p = 0$ or 1, it becomes the more familiar reflected process. The following proposition gives the existence and uniqueness of the strong solution of the SDE (1):

Proposition 2.1. *The above generalized skew Vasicek model with discontinuous drift admits a unique strong solution.*

Proof. Define

$$\nu(A) = \int_A \frac{k(\theta_1 \mathbb{1}_{\{r_t<a_1\}} + \theta_2 \mathbb{1}_{\{r_t\geq a_1\}} - y)}{\sigma^2} \mathrm{d}y + (2p-1)\delta_{a_2}(A),$$

where $\delta_{a_2}(\cdot)$ denotes the Delta function. For every $N \geq 1$, ν is a finite signed measure on $\mathcal{B}([-N, N])$, and satisfies $|\nu(\{x\})| < 1$. Thus, the following equation is satisfied

$$\begin{aligned}
& r_0 + \int_{\mathbb{R}} \hat{L}_t^r(y)\nu(\mathrm{d}y) + \int_0^t \sigma \mathrm{d}W_s \\
&= r_0 + \int_{\mathbb{R}} \hat{L}_t^r(y) \left[\frac{k(\theta_1 \mathbb{1}_{\{r_t<a_1\}} + \theta_2 \mathbb{1}_{\{r_t\geq a_1\}} - y)}{\sigma^2} \mathrm{d}y + (2p-1)\delta_{a_2}(\mathrm{d}y) \right] + \int_0^t \sigma \mathrm{d}W_s \\
&= r_0 + \int_{\mathbb{R}} \hat{L}_t^r(y) \frac{k(\theta_1 \mathbb{1}_{\{r_t<a_1\}} + \theta_2 \mathbb{1}_{\{r_t\geq a_1\}} - y)}{\sigma^2} \mathrm{d}y + (2p-1) \int_{\mathbb{R}} \hat{L}_t^r(y)\delta_{a_2}(\mathrm{d}y) + \int_0^t \sigma \mathrm{d}W_s \\
&= r_0 + \int_0^t \frac{k(\theta_1 \mathbb{1}_{\{r_t<a_1\}} + \theta_2 \mathbb{1}_{\{r_t\geq a_1\}} - r_s)}{\sigma^2} \mathrm{d}\langle r \rangle_s + (2p-1)\hat{L}_t^r(a_2) + \int_0^t \sigma \mathrm{d}W_s \\
&= r_0 + \int_0^t k(\theta_1 \mathbb{1}_{\{r_t<a_1\}} + \theta_2 \mathbb{1}_{\{r_t\geq a_1\}} - r_s)\mathrm{d}s + \int_0^t \sigma \mathrm{d}W_s + (2p-1)\hat{L}_t^r(a_2) \\
&= r_t.
\end{aligned}$$

The third equality holds due to occupation times formula (see e.g. Revuz & Yor (1999)), which only requires that the function is twice differentiable. In other words, the second-order derivative is not necessarily continuous. Now set

$$g(x) = \begin{cases} \exp\left(\frac{k}{\sigma^2}x^2 - \frac{2k\left(\theta_1 \mathbb{1}_{\{r_t<a_1\}} + \theta_2 \mathbb{1}_{\{r_t\geq a_1\}}\right)}{\sigma^2} x \right), & x < a_2 \\ \frac{1-p}{p} \exp\left(\frac{k}{\sigma^2}x^2 - \frac{2k\left(\theta_1 \mathbb{1}_{\{r_t<a_1\}} + \theta_2 \mathbb{1}_{\{r_t\geq a_1\}}\right)}{\sigma^2} x \right), & x \geq a_2 \end{cases} \tag{2}$$

and

$$G(r) = \int_0^r g(y)\mathrm{d}y, \quad x \in \mathbb{R} \tag{3}$$

Note that the integral $\int_0^\infty e^{\hat{a}y^2+\hat{b}y+\hat{c}}\mathrm{d}y$ ($\hat{a} \neq 0$) is finite if and only if $\hat{a} < 0$. In our case, where $\hat{a}$ is equal to $\frac{k}{\sigma^2} > 0$, this leads to $G(+\infty) = +\infty$ and $G(-\infty) = -\infty$. Consequently, the solution does not explode according to Proposition 4.34 in Engelbert & Schmidt (1991).

Now, for any real function, introduce the following two sets:

$$\begin{aligned}
N_f &= \{x \in \mathbb{R} : f(x) = 0\}, \\
E_f &= \{x \in \mathbb{R} : \int_A \frac{1}{f^2(y)}\mathrm{d}y = +\infty \text{ for all open sets } A \text{ containing } x\}.
\end{aligned}$$

Obviously, $N_\sigma = \varnothing$ and $E_\sigma = \varnothing$, by Theorem 4.35, 4.37 and Corollary in Engelbert & Schmidt (1991), (1) possesses a unique strong solution $(r_t, \mathcal{F}_t)$ which is a strong Markov process. □

Note that the long-term mean switching between regimes is controlled by the *threshold level* a_1, whereas the skew level a_2 determines where the local time can exert influence on the process. Theoretically, a_1 and a_2 can share the same value (confer Table 4 and Table 9). One of the reasons for choosing a_1 different from a_2 is that it enables to differentiate the effects of the discontinuous drift and the local time. This feature of the model is important when one wishes to take into consideration the effects of the local time component for very large or very small values of a_2.

When considering tree lattice construction of the generalized skew Vasicek model with discontinuous drift, the major obstacle is actually the local time in (1). Although the drift term is discontinuous, it is not that essential in the tree structure. As a result, in order to get rid of the local time, similar to Zhuo *et al.* (2016a) and Zhuo *et al.* (2016b), we set $Y_t = g(r_t)$ where

$$Y_t = g(x) := \begin{cases} p(x - a_2) + a_2 & \text{if} \quad x < a_2, \\ (1-p)(x - a_2) + a_2 & \text{if} \quad x \geq a_2. \end{cases} \tag{4}$$

Proposition 2.2. *The transformed process $Y_t = g(r_t)$ satisfies the following stochastic differential equation*

$$\mathrm{d}Y_t = \tilde{\mu}(Y_t)\mathrm{d}t + \tilde{\sigma}(Y_t)\mathrm{d}W_t, \tag{5}$$

where $\tilde{\mu}(Y_t)$ and $\tilde{\sigma}(Y_t)$ are defined respectively by

$$\tilde{\mu}(Y_t) := \begin{cases} \tilde{\mu}_1(Y_t) & \textit{if} \quad a_1 < a_2, \\ \tilde{\mu}_2(Y_t) & \textit{if} \quad a_1 \geq a_2, \end{cases} \qquad \tilde{\sigma}(Y_t) := \begin{cases} p\sigma & \textit{if} \quad Y_t < a_2, \\ (1-p)\sigma & \textit{if} \quad Y_t \geq a_2, \end{cases} \tag{6}$$

with

$$\tilde{\mu}_1(Y_t) = \begin{cases} k(p\theta_1 + (1-p)a_2 - Y_t) & \textit{if} \quad Y_t < pa_1 + (1-p)a_2, \\ k(p\theta_2 + (1-p)a_2 - Y_t) & \textit{if} \quad pa_1 + (1-p)a_2 \leq Y_t < a_2, \\ k((1-p)\theta_2 + pa_2 - Y_t) & \textit{if} \quad Y_t \geq a_2, \end{cases}$$

$$\tilde{\mu}_2(Y_t) = \begin{cases} k(p\theta_1 + (1-p)a_2 - Y_t) & \textit{if} \quad Y_t < a_2, \\ k((1-p)\theta_1 + pa_2 - Y_t) & \textit{if} \quad a_2 \leq Y_t < (1-p)a_1 + pa_2, \\ k((1-p)\theta_2 + pa_2 - Y_t) & \textit{if} \quad Y_t \geq (1-p)a_1 + pa_2. \end{cases}$$

Proof. Since $g(\cdot)$ defined in (4) is the difference of convex functions, application of the generalized Itô formula (see, for example, Protter (2005), page 271) to $Y_t = g(r_t)$ yields

$$\begin{aligned} Y_t =& Y_0 + \int_0^t g'(r_s)\mathrm{d}r_s + \frac{1}{2}\int_0^t g''(r_s)\mathrm{d}\langle r\rangle_s + \frac{1}{2}\left[g'(a_2+) - g'(a_2-)\right]\hat{L}_t^r(a_2) \\ =& Y_0 + \int_0^t g'(r_s)k\left(\theta_1 \mathbb{1}_{\{r_s<a_1\}} + \theta_2 \mathbb{1}_{\{r_s\geq a_1\}} - r_s\right)\mathrm{d}s + \int_0^t g'(r_s)\sigma\mathrm{d}W_s \\ &+ \int_0^t g'(r_s)(2p-1)\mathrm{d}\hat{L}_s^r(a_2) + \frac{1}{2}(1-p-p)\hat{L}_t^r(a_2) \end{aligned}$$

$$=Y_0+\int_0^t g'(r_s)k\left(\theta_1\mathbb{1}_{\{r_s<a_1\}}+\theta_2\mathbb{1}_{\{r_s\geq a_1\}}-r_s\right)\mathrm{d}s+\int_0^t g'(r_s)\sigma\mathrm{d}W_s.$$

The last equality follows from

$$\begin{aligned}
&\int_0^t g'(r_s)(2p-1)\mathrm{d}\hat{L}_s^r(a_2)+\frac{1}{2}\left(1-p-p\right)\hat{L}_t^r(a_2)\\
=&g'(a_2)(2p-1)\hat{L}_t^r(a_2)+\frac{1}{2}\left(1-2p\right)\hat{L}_t^r(a_2)\\
=&\frac{1}{2}\left[g'(a_2+)+g'(a_2-)\right](2p-1)\hat{L}_t^r(a_2)+\frac{1}{2}\left(1-2p\right)\hat{L}_t^r(a_2)\\
=&\frac{1}{2}\left(1-p+p\right)(2p-1)\hat{L}_t^r(a_2)+\frac{1}{2}\left(1-2p\right)\hat{L}_t^r(a_2)\\
=&0.
\end{aligned}$$

Thus the process Y_t satisfies the following stochastic differential equation

$$\begin{aligned}
\mathrm{d}Y_t&=g'(r_t)k\left(\theta_1\mathbb{1}_{\{r_t<a_1\}}+\theta_2\mathbb{1}_{\{r_t\geq a_1\}}-r_t\right)\mathrm{d}t+g'(r_t)\sigma\mathrm{d}W_t \qquad (7)\\
&=\begin{cases}
pk\left(\theta_1\mathbb{1}_{\{r_t<a_1\}}+\theta_2\mathbb{1}_{\{r_t\geq a_1\}}-r_t\right)\mathrm{d}t+p\sigma\mathrm{d}W_t & \text{if}\quad r_t<a_2,\\
(1-p)\,k\left(\theta_1\mathbb{1}_{\{r_t<a_1\}}+\theta_2\mathbb{1}_{\{r_t\geq a_1\}}-r_t\right)\mathrm{d}t+(1-p)\,\sigma\mathrm{d}W_t & \text{if}\quad r_t\geq a_2.
\end{cases}
\end{aligned}$$

Specifically, if $a_1<a_2$, (7) becomes

$$\begin{aligned}
\mathrm{d}Y_t&=g'(r_t)k\left(\theta_1\mathbb{1}_{\{r_t<a_1\}}+\theta_2\mathbb{1}_{\{r_t\geq a_1\}}-r_t\right)\mathrm{d}t+g'(r_t)\sigma\mathrm{d}W_t\\
&=\begin{cases}
pk\left(\theta_1-r_t\right)\mathrm{d}t+p\sigma\mathrm{d}W_t & \text{if}\quad r_t<a_1,\\
pk\left(\theta_2-r_t\right)\mathrm{d}t+p\sigma\mathrm{d}W_t & \text{if}\quad a_1\leq r_t<a_2,\\
(1-p)k\left(\theta_2-r_t\right)\mathrm{d}t+(1-p)\sigma\mathrm{d}W_t & \text{if}\quad r_t\geq a_2,
\end{cases}\\
&=\begin{cases}
k\left(p\theta_1+(1-p)a_2-Y_t\right)\mathrm{d}t+p\sigma\mathrm{d}W_t & \text{if}\quad Y_t<pa_1+(1-p)a_2,\\
k\left(p\theta_2+(1-p)a_2-Y_t\right)\mathrm{d}t+p\sigma\mathrm{d}W_t & \text{if}\quad pa_1+(1-p)a_2\leq Y_t<a_2,\\
k\left((1-p)\theta_2+pa_2-Y_t\right)\mathrm{d}t+(1-p)\sigma\mathrm{d}W_t & \text{if}\quad Y_t\geq a_2,
\end{cases}\\
&=\tilde{\mu}_1(Y_t)\mathrm{d}t+\tilde{\sigma}_1(Y_t)\mathrm{d}W_t, \qquad (8)
\end{aligned}$$

and if $a_1\geq a_2$, (7) becomes

$$\begin{aligned}
\mathrm{d}Y_t&=g'(r_t)k\left(\theta_1\mathbb{1}_{\{r_t<a_1\}}+\theta_2\mathbb{1}_{\{r_t\geq a_1\}}-r_t\right)\mathrm{d}t+g'(r_t)\sigma\mathrm{d}W_t\\
&=\begin{cases}
pk\left(\theta_1-r_t\right)\mathrm{d}t+p\sigma\mathrm{d}W_t & \text{if}\quad r_t<a_2,\\
(1-p)k\left(\theta_1-r_t\right)\mathrm{d}t+(1-p)\sigma\mathrm{d}W_t & \text{if}\quad a_2\leq r_t<a_1,\\
(1-p)k\left(\theta_2-r_t\right)\mathrm{d}t+(1-p)\sigma\mathrm{d}W_t & \text{if}\quad r_t\geq a_1,
\end{cases}\\
&=\begin{cases}
k\left(p\theta_1+(1-p)a_2-Y_t\right)\mathrm{d}t+p\sigma\mathrm{d}W_t & \text{if}\quad Y_t<a_2,\\
k\left((1-p)\theta_1+pa_2-Y_t\right)\mathrm{d}t+(1-p)\sigma\mathrm{d}W_t & \text{if}\quad a_2\leq Y_t<(1-p)a_1+pa_2,\\
k\left((1-p)\theta_2+pa_2-Y_t\right)\mathrm{d}t+(1-p)\sigma\mathrm{d}W_t & \text{if}\quad Y_t\geq(1-p)a_1+pa_2,
\end{cases}\\
&=\tilde{\mu}_2(Y_t)\mathrm{d}t+\tilde{\sigma}_2(Y_t)\mathrm{d}W_t. \qquad (9)
\end{aligned}$$

where the third equality in (8) or (9) holds due to the inverse transform between r_t and Y_t, which

is given by

$$r_t = g^{-1}(Y_t) = \begin{cases} \dfrac{1}{p}(Y_t - a_2) + a_2 & \text{if} \quad Y_t < a_2, \\ \dfrac{1}{1-p}(Y_t - a_2) + a_2 & \text{if} \quad Y_t \geq a_2. \end{cases} \tag{10}$$

Hence the result follows. □

We observe that the threshold level a_1 in discontinuous drift scheme only affects the drift component $\tilde{\mu}(Y_t)$ of the transformed process Y_t, while the diffusion component $\tilde{\sigma}(Y_t)$ remains unchanged with respect to different values of a_1. As we will see below, the key element of tree construction is the diffusion coefficient, whereas the discontinuity of the drift process mainly exerts an influence on the expected mean of different grids. Therefore, we do not need to regard the process Y_t as a three-piece piecewise process, what matters for tree construction is the diffusion functions of Y_t. In essence, the diffusion function $\tilde{\sigma}(Y_t)$ in (6) is a two-piece piecewise process, that's why we only have two subregions in the following piecewise lattice construction.

Notably, compared to Zhuo *et al.* (2016a) and Zhuo *et al.* (2016b) who both use two transforms to their corresponding skew-extended models, we only need one transform. This is simpler and more efficient. Because the tree is built based on the transformed process, one transform generally results in smaller pricing errors than two transforms, as shown in Zhuo *et al.* (2016b) whose two-transform tree approach converges slightly slower than the one-transform tree approach in Beliaeva & Nawalkha (2012).

3. The Proposed Piecewise Binomial Lattice

In this section, we will investigate the binomial lattice construction by using the one-to-one transformed process Y_t defined in (5). Even though we only build Y_t-tree, the tree for r_t can be easily derived from the relation (10).

We decompose the binomial construction for Y_t-tree in three steps: the first step focuses on the decision of a proxy/substitute for the skew level a_2; the second step designs nonuniform jump sizes for different regimes; and the third step gives a simple treatment at the proxy skew level, so that the tree would recombine in all regimes.

Step 1: Definition of the proxy skew level $\tilde{a}_2$

Let y_t represent the discrete value of Y_t at time t. In order to construct the binomial tree for y_t, we first define a proxy (or substitute) $\tilde{a}_2$ for the real skew level a_2 by

$$\tilde{a}_2 := \begin{cases} y_0 + Z_0 p\sigma\sqrt{\Delta t} & \text{if} \quad y_0 < a_2, \\ y_0 - Z_0(1-p)\sigma\sqrt{\Delta t} & \text{if} \quad y_0 \geq a_2, \end{cases} \tag{11}$$

where y_0 denotes the starting value of the y_t-tree, computed by using the initial value of the short rate r_0 according to (4). Δt is the time step and Z_0 is computed as follows:

$$Z_0 = INT\left(\frac{|y_0 - a_2|}{\tilde{\sigma}(y_0)\sqrt{\Delta t}}\right), \tag{12}$$

with $INT(\cdot)$ be the integer value function. It is noteworthy that, as the time step Δt approaches zero, the proxy $\tilde{a}_2$ converges to the real a_2. Hence, by such construction, we claim that $\tilde{a}_2$ is a proxy for a_2. The importance of introducing the substitute $\tilde{a}_2$ will be made clear in the next step.

Step 2: Construction of the binomial lattice when $y_t \neq \tilde{a}_2$

Now we consider the binomial tree construction in detail. We call *regular node* for any node on the grid of the binomial tree that does not lie at the proxy skew level $\tilde{a}_2$. The up and down nodes of a regular node y_t are respectively given by

$$\begin{aligned} y_u &:= y_t + \tilde{\sigma}(y_t)\sqrt{\Delta t}, \\ y_d &:= y_t - \tilde{\sigma}(y_t)\sqrt{\Delta t}, \end{aligned} \tag{13}$$

where $\tilde{\sigma}(y_t)$ is the piecewise volatility of y_t, given by (6), in which a_2 is replaced by $\tilde{a}_2$.

Notably, as shown in Fig. 1, the jump size $\tilde{\sigma}(y_t)\sqrt{\Delta t}$ of y_t varies according to the regimes. In particular, if y_t is less than $\tilde{a}_2$ the jump size is $p\sigma\sqrt{\Delta t}$, and if y_t is larger than $\tilde{a}_2$ the jump size is $(1-p)\sigma\sqrt{\Delta t}$. Additionally, when $p < 0.5$, the left panel of Fig. 1 shows that the jump size $(1-p)\sigma\sqrt{\Delta t}$ of y_t in the high rate regime (above the proxy skew level $\tilde{a}_2$) is larger than the jump size $p\sigma\sqrt{\Delta t}$ in the low rate regime (below the proxy skew level $\tilde{a}_2$). When $p > 0.5$, the contrary effects are observed as illustrated in the right panel of Fig. 1.

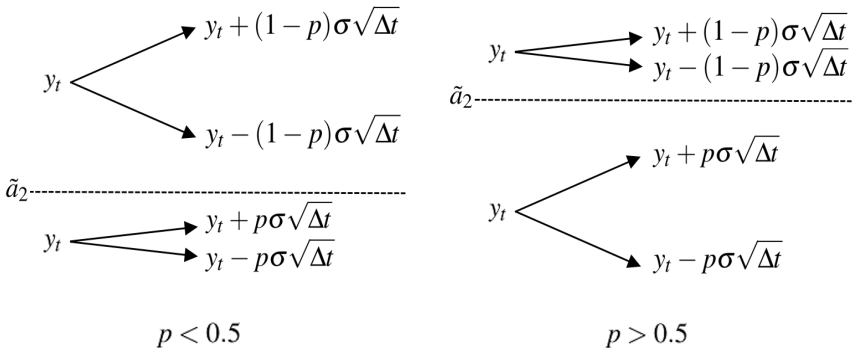

Figure 1: Regular nodes for the binomial tree. When $p < 0.5$, the left panel depicts larger jump-size node in the high rate regime and smaller jump-size node in the low rate regime. When $p > 0.5$, the right panel depicts larger jump-size node in the low rate regime and smaller jump-size node in the high rate regime.

The nonuniform jump sizes in different regimes are designed to allow for the matching of the instantaneous variance of the piecewise process Y_t. For instance, the volatility of Y_t is $p\sigma$ in the low rate regime. Hence we require the jump size to be $p\sigma\sqrt{\Delta t}$ so as to match the instantaneous variance $p^2\sigma^2\Delta t$.

Moreover, the probabilities of the up and down nodes are chosen such that the expected value of the jump sizes of the process y_t in the next time step is equal to its drift, that is,

$$p_u \cdot (y_u - y_t) + p_d \cdot (y_d - y_t) = \tilde{\mu}(y_t)\Delta t,$$

where $\tilde{\mu}(y_t)$ is the piecewise drift of y_t given by (6) and depends on the real skew level a_2. A simple calculation leads to

$$\begin{aligned} p_u &= \frac{1}{2} + \frac{1}{2}\frac{\tilde{\mu}(y_t)}{\tilde{\sigma}(y_t)}\sqrt{\Delta_t}, \\ p_d &= \frac{1}{2} - \frac{1}{2}\frac{\tilde{\mu}(y_t)}{\tilde{\sigma}(y_t)}\sqrt{\Delta_t}. \end{aligned} \tag{14}$$

Remark 3.0.1. *We do not replace a_2 with $\tilde{a}_2$ in $\tilde{\mu}(y_t)$, because $\tilde{\mu}(y_t)$ are only used to derive the probabilities, rather than to define the jump structure. Furthermore, even if $\tilde{\sigma}(y_t)$ in (14) is a proxy for the volatility (because a_2 is replaced by $\tilde{a}_2$), we still keep the real skew level a_2 in $\tilde{\mu}(y_t)$ such that the precise (instead of proxy) drift component is used and the proxy errors are only due to $\tilde{\sigma}(y_t)$ in the computation of the probabilities. Let us mention that the proxy errors in (13) and (14), produced by the volatility $\tilde{\sigma}(y_t)$ in which a_2 is replaced by $\tilde{a}_2$, only happen around the level a_2 and become negligible when $\tilde{a}_2$ is equal or very close to a_2.*

Next, we discuss the importance of the proxy skew level $\tilde{a}_2$ given by (11). As indicated earlier, at any given node (including the initial node y_0), the jump size varies according to the regimes. If the initial node y_0 is greater than the proxy skew level $\tilde{a}_2$ (and also the real skew level a_2), then y_0

jumps up and down with grid size $(1-p)\sigma\sqrt{\Delta t}$. Therefore, the level $\tilde{a}_2$ defined in the second piece of (11) is the downward jump node from y_0 closest to the real skew level a_2. To ensure that the tree recombines at the future nodes, we replace the real level a_2 by its closest substitute $\tilde{a}_2$. The error between $\tilde{a}_2$ and a_2 converges to zero as Δt approaches zero. Similar arguments are applied when y_0 is less than the real skew level a_2.

Step 3: Construction of the binomial lattice when $y_t = \tilde{a}_2$

It follows from (11) that $\tilde{a}_2$ must be on the grid of the binomial tree. Hence starting with an initial point y_0, the tree will eventually touch the proxy skew level $\tilde{a}_2$. When the process y_t touches $\tilde{a}_2$ (independently from which side), we claim that the jump size should be artificially adjusted in the time step after so as to recombine.

In fact, when y_t is equal to $\tilde{a}_2$, the up and down moves of the process y_t in the next time step are given by

$$\begin{aligned} y_u &:= y_t + (1-p)\sigma\sqrt{\Delta t}, \\ y_d &:= y_t - p\sigma\sqrt{\Delta t}. \end{aligned} \tag{15}$$

In this manner, the up jumps y_u is on the grid of the high rate regime (in which the jump size is $(1-p)\sigma\sqrt{\Delta t}$), and the down jumps y_d is on the grid of the low rate regime (in which the jump size is $p\sigma\sqrt{\Delta t}$), so that the tree will recombine at the future nodes. The basic nodes at the proxy skew level $\tilde{a}_2$ are shown in Fig. 2.

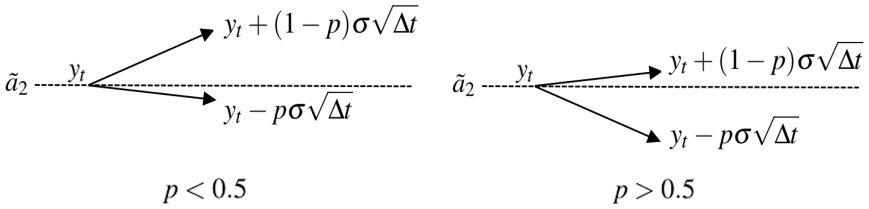

Figure 2: Nodes at the proxy skew level $\tilde{a}_2$ for the binomial tree. When $p < 0.5$, the left panel illustrates larger jump-size upward node and smaller jump-size downward node. When $p > 0.5$, the right panel illustrates larger jump-size downward node and smaller jump-size upward node.

Only the drift of the y_t process is matched in this step. Once more, the probabilities of up and down nodes are computed such that the expected value of jumps equals the corresponding drift, in other words,

$$p_u \cdot (1-p)\sigma\sqrt{\Delta t} + p_d \cdot (-p\sigma\sqrt{\Delta t}) = \tilde{\mu}(y_t)\Delta t.$$

A simple calculation reveals that

$$\begin{aligned} p_u &= p + \frac{\tilde{\mu}(y_t)}{\sigma}\sqrt{\Delta t}, \\ p_d &= 1 - p - \frac{\tilde{\mu}(y_t)}{\sigma}\sqrt{\Delta t}. \end{aligned} \tag{16}$$

Fig. 3 depicts the typical proposed binomial tree. We discard the real skew level a_2, which is the gray dashed line in Fig. 3. Instead, the proxy skew level $\tilde{a}_2$ (the black dashed line) is used to divide nonuniform jump sizes, $p\sigma\sqrt{\Delta t}$ and $(1-p)\sigma\sqrt{\Delta t}$. Meanwhile, the jump size at the proxy skew level $\tilde{a}_2$ is modified to fit different grid sizes in different regimes.

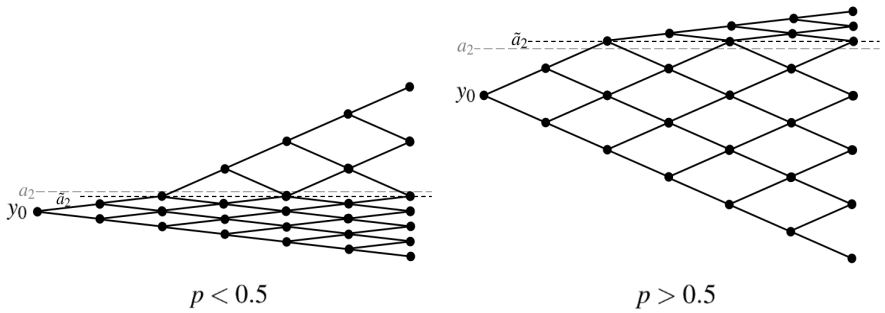

Figure 3: The proposed binomial tree. When $p < 0.5$, the left panel shows a general piecewise binomial tree structure in which larger jump-size nodes are located in the high rate regime and smaller jump-size nodes are located in the low rate regime. When $p > 0.5$, the right panel shows a general piecewise binomial tree structure in which larger jump-size nodes are located in the low rate regime and smaller jump-size nodes are located in the high rate regime.

This piecewise binomial lattice is motivated by the tree method in Zhuo *et al.* (2016a), who apply two transforms to the skew CEV model and propose a similar piecewise binomial tree method. The differences in this paper are that, we only use one transform and our jump size is related to the volatility parameter σ, which does not appear in the jump size of the tree in Zhuo *et al.* (2016a).

4. The Proposed Piecewise Trinomial Lattice

In this section, we go one step further by extending the piecewise binomial lattice method to the trinomial case. The main difference between the trinomial lattice and the binomial lattice is that, in the former case, the discrete value y_t of Y_t, can either go up, down, or stay at the same level in the next node.

We will now explore the trinomial lattice construction for the transformed process Y_t given by (5). The trinomial construction is decomposed in four steps: the first step defines the proxy skew level $\hat{a}_2$; the second step proposes nonuniform jump sizes for different regimes, similar to those of the

binomial lattice approach in the previous section; the third step investigates the node modification at the proxy skew level, while the fourth step determines the value of the adjustment parameter b. Then, the tree for r_t can also be obtained by using the relation between Y_t and r_t in (10).

Step 1: Definition of the proxy skew level $\hat{a}_2$

Let y_t be the discrete value of Y_t at time t, and define the proxy skew level $\hat{a}_2$ as follows:

$$\hat{a}_2 := \begin{cases} y_0 + Z_0 bp\sigma\sqrt{\Delta t} & \text{if} \quad y_0 < a_2, \\ y_0 - Z_0 b(1-p)\sigma\sqrt{\Delta t} & \text{if} \quad y_0 \geq a_2, \end{cases} \tag{17}$$

where y_0 is the starting value of the y_t-tree, computed by using the initial short rate r_0 according to (4). Z_0 is an integer value given by

$$Z_0 = INT\left(\frac{|y_0 - a_2|}{b\tilde{\sigma}(y_0)\sqrt{\Delta t}}\right), \tag{18}$$

where b is an adjustment parameter, which is a constant strictly greater than 1 to adjust the jump size. Let us mention that the main difference between $\tilde{a}_2$ given by (11) and $\hat{a}_2$ given by (17) is the presence of the constant b in the definition of $\hat{a}_2$. For $b = 1$, $\tilde{a}_2$ and $\hat{a}_2$ coincide. We will later discuss the determination of b in step 4.

Step 2: Construction of the trinomial lattice when $y_t \neq \hat{a}_2$

In this step, we study nodes which are away from the proxy skew level $\hat{a}_2$, i.e., nodes in the high rate regime (larger than $\hat{a}_2$) and nodes in the low rate regime (smaller than $\hat{a}_2$). To be more precise, for any given node y_t, the up, middle and down nodes are defined as follows:

$$\begin{aligned} y_u &:= y_t + b\tilde{\sigma}(y_t)\sqrt{\Delta t}, \\ y_m &:= y_t, \\ y_d &:= y_t - b\tilde{\sigma}(y_t)\sqrt{\Delta t}, \end{aligned} \tag{19}$$

where $\tilde{\sigma}(y_t)$ is the piecewise volatility of y_t defined in (6), in which a_2 is replaced by $\hat{a}_2$.

The jump size $b\tilde{\sigma}(y_t)\sqrt{\Delta t}$ for the trinomial tree is equivalent to that for the binomial tree up to the constant b. The setting of $b > 1$ stems from the classical trinomial method restriction; we refer the reader to, for example, Boyle (1988), Kamrad & Ritchken (1991) for more details. Similarly, Fig.4 depicts the regular nodes for the trinomial tree.

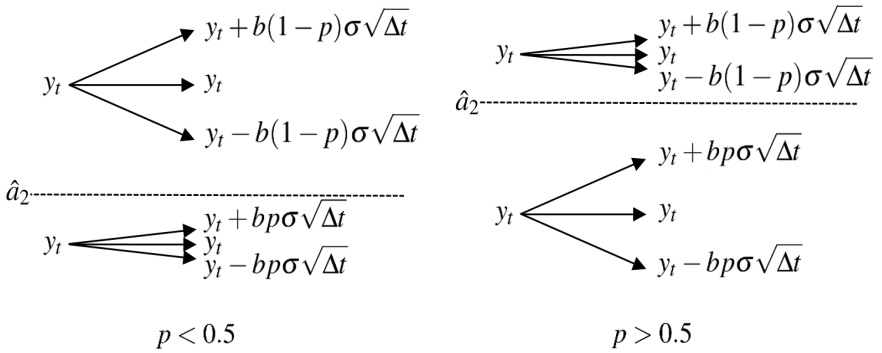

Figure 4: Regular nodes for the trinomial tree. When $p < 0.5$, the left panel depicts larger jump-size node in the high rate regime and smaller jump-size node in the low rate regime. When $p > 0.5$, the right panel depicts larger jump-size node in the low rate regime and smaller jump-size node in the high rate regime.

In order to match the instantaneous mean and variance of the process y_t, using the three nodes in (19), the trinomial probabilities are computed by solving the following system of three equations:

$$\begin{aligned} &\sum_{i=u,m,d} p_i(y_i - y_t) = \tilde{\mu}(y_t)\Delta t, \\ &\sum_{i=u,m,d} p_i(y_i - y_t)^2 = [\tilde{\mu}(y_t)\Delta t]^2 + \tilde{\sigma}^2(y_t)\Delta t, \\ &\sum_{i=u,m,d} p_i = 1, \end{aligned} \tag{20}$$

where $\tilde{\mu}(y_t)$ is the piecewise drift of y_t given by (6) and depends on the real skew level a_2; $\tilde{\sigma}(y_t)$ is the piecewise volatility of y_t given by (6) in which a_2 is replaced by $\hat{a}_2$.

One of the main features of using trinomial tree is that it enables exact matching of the mean and variance of the y_t-process. This is in general not possible in a binomial construction. More precisely, the trinomial tree can match the exact variance $[\tilde{\mu}(y_t)\Delta t]^2 + \tilde{\sigma}^2(y_t)\Delta t$, whereas the binomial tree only matches the approximated variance $\tilde{\sigma}^2(y_t)\Delta t$ and ignores the high order term $[\tilde{\mu}(y_t)\Delta t]^2$.

The solution (p_u, p_m, p_d) to the system of (20) is given by

$$\begin{aligned} p_u &= \frac{1}{2b^2} + \frac{1}{2b}\frac{\tilde{\mu}(y_t)}{\tilde{\sigma}(y_t)}\sqrt{\Delta t} + \frac{1}{2b^2}\frac{\tilde{\mu}^2(y_t)}{\tilde{\sigma}^2(y_t)}\Delta t, \\ p_m &= 1 - \frac{1}{b^2} - \frac{1}{b^2}\frac{\tilde{\mu}^2(y_t)}{\tilde{\sigma}^2(y_t)}\Delta t, \\ p_d &= \frac{1}{2b^2} - \frac{1}{2b}\frac{\tilde{\mu}(y_t)}{\tilde{\sigma}(y_t)}\sqrt{\Delta t} + \frac{1}{2b^2}\frac{\tilde{\mu}^2(y_t)}{\tilde{\sigma}^2(y_t)}\Delta t. \end{aligned} \tag{21}$$

Step 3: Construction of the trinomial lattice when $y_t = \hat{a}_2$

In this step, the jump sizes of upward, horizontal, and downward nodes of the y_t-process are modified when it stays at the proxy skew level $\hat{a}_2$, so that the nodes in the future time steps can

recombine in all regimes. To achieve this, the up, middle and down moves of the process y_t at the proxy skew level $\hat{a}_2$ are given as follows:

$$\begin{aligned} y_u &:= y_t + b(1-p)\sigma\sqrt{\Delta t}, \\ y_m &:= y_t, \\ y_d &:= y_t - bp\sigma\sqrt{\Delta t}. \end{aligned} \tag{22}$$

Fig. 5 shows the nodes at the proxy skew level $\hat{a}_2$. As shown in the previous step 2, the next jump size of the up node y_u is $b(1-p)\sigma\sqrt{\Delta t}$, whereas that of the down node y_d is $bp\sigma\sqrt{\Delta t}$. In this setting, their future nodes recombine. More precisely, y_u (resp. y_d) either jumps into high (resp. low) rate regime with jump size $b(1-p)\sigma\sqrt{\Delta t}$ (resp. $bp\sigma\sqrt{\Delta t}$), which will recombine in its regime (according to step 2); or jumps at the proxy skew level $\hat{a}_2$, which will recombine one step further using the modified jump sizes in step 3.

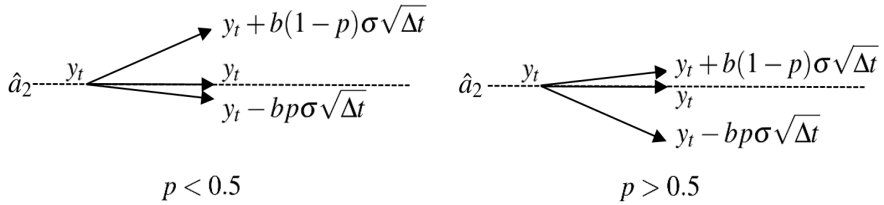

Figure 5: Nodes at the proxy skew level $\hat{a}_2$ for the trinomial tree. When $p < 0.5$, the left panel illustrates larger jump-size upward node and smaller jump-size downward node. When $p > 0.5$, the right panel illustrates larger jump-size downward node and smaller jump-size upward node.

By matching the instantaneous drift and variance relation in (20) and using (y_u, y_m, y_d) in (22), it is easy to show that the probabilities of the up, middle and down nodes at the proxy skew level $\hat{a}_2$ are respectively given by

$$\begin{aligned} p_u &= \frac{1}{(1-p)b^2}\frac{\tilde{\sigma}^2(y_t)}{\sigma^2} + \frac{p}{(1-p)b}\frac{\tilde{\mu}(y_t)}{\sigma}\sqrt{\Delta t} + \frac{1}{(1-p)b^2}\frac{\tilde{\mu}^2(y_t)}{\sigma^2}\Delta t, \\ p_m &= 1 - \frac{1}{p(1-p)b^2}\frac{\tilde{\sigma}^2(y_t)}{\sigma^2} - \frac{2p-1}{p(1-p)b}\frac{\tilde{\mu}(y_t)}{\sigma}\sqrt{\Delta t} - \frac{1}{p(1-p)b^2}\frac{\tilde{\mu}^2(y_t)}{\sigma^2}\Delta t, \\ p_d &= \frac{1}{pb^2}\frac{\tilde{\sigma}^2(y_t)}{\sigma^2} - \frac{1-p}{pb}\frac{\tilde{\mu}(y_t)}{\sigma}\sqrt{\Delta t} + \frac{1}{pb^2}\frac{\tilde{\mu}^2(y_t)}{\sigma^2}\Delta t. \end{aligned} \tag{23}$$

Step 4: Determination of the adjustment parameter b

Let us now discuss the process of finding the value of b. Notice that, for jump probabilities when $y_t \neq \hat{a}_2$ in (21), if $b = 1$, then $p_m < 0$. This is neither realistic nor acceptable. Besides, if $b \to \infty$, then $p_m \to 1$, in other words, the process y_t will stay at the same level in the next step. A typical

value of b used by researchers is $\sqrt{3}$ (see e.g., Hull & White (1994)). Setting $b = \sqrt{3}$ is a good choice for (21). In this case, as the time step Δt approaches zero, the probabilities of the middle node p_m is close to $1 - 1/b^2 = 2/3$.

However, things are different if the skew probability p takes value smaller than $\frac{1}{b^2+1}$ when $y_t = \hat{a}_2$ in (23). For example, when $p = 0.2$, setting $b = \sqrt{3}$ and as $\sqrt{\Delta t} \to 0$ in (23), we have

$$
\begin{aligned}
p_u &\approx \frac{1}{(1-p)b^2}\frac{\tilde{\sigma}^2(\hat{a}_2)}{\sigma^2} = \frac{1-p}{b^2} = \frac{4}{15}, \\
p_m &\approx 1 - \frac{1}{p(1-p)b^2}\frac{\tilde{\sigma}^2(\hat{a}_2)}{\sigma^2} = 1 - \frac{1-p}{p}\frac{1}{b^2} = -\frac{1}{3} < 0, \\
p_d &\approx \frac{1}{pb^2}\frac{\tilde{\sigma}^2(\hat{a}_2)}{\sigma^2} = \frac{(1-p)^2}{pb^2} = \frac{16}{15} > 1,
\end{aligned}
$$

leading to negative probability or probability greater than 1. This violates the general condition for probabilities. Therefore, one should carefully choose the value of b to have reasonable probabilities p_u, p_m and p_d when $y_t = \hat{a}_2$ in (23). To simplify calculations, the terms which are of the order $O(\sqrt{\Delta_t})$ or $o(\sqrt{\Delta_t})$ in p_u, p_m and p_d are ignored. In fact, an initial setting of $b_0 = \max(\sqrt{\frac{1-p}{p}}, \sqrt{3})$ will basically ensure that $0 \le p_u, p_m, p_d \le 1$ in (23).[1]

In addition, the main pricing errors are from the difference between the proxy skew level and the real skew level. For the binomial tree, we can only reduce errors by properly choosing the time step Δt in such a way that $\tilde{a}_2$ is equal or very close to a_2. Whereas for the trinomial trees, an extra degree of freedom allows us to adjust the value of b. Formally, we define b as follows:

$$
b := \begin{cases} b_0 & \text{if} \quad |y_0 - a_2| \le b_0\tilde{\sigma}(y_0)\sqrt{\Delta t}, \\ \dfrac{|y_0 - a_2| / \left(\tilde{\sigma}(y_0)\sqrt{\Delta t}\right)}{FLOOR\left(\frac{|y_0-a_2|}{b_0\tilde{\sigma}(y_0)\sqrt{\Delta t}}\right)} & \text{if} \quad |y_0 - a_2| > b_0\tilde{\sigma}(y_0)\sqrt{\Delta t}, \end{cases} \tag{24}
$$

where $FLOOR(\cdot)$ is the integer value function, rounded down. By definition, we regard b_0 as the lower bound for b. With an initial node y_0 which is at least $b_0\tilde{\sigma}(y_0)\sqrt{\Delta t}$ distance away from a_2, the jump size is expanded to $b\tilde{\sigma}(y_0)\sqrt{\Delta t}$ such that the Y_t-tree will exactly hit the real skew level a_2. By doing so, the proxy level $\hat{a}_2$ defined in (17) is precisely equal to the real skew level a_2, resulting in less pricing errors and more stable prices with respect to the number of steps. However, when y_0 is close to a_2, we still let $b = b_0$ and keep the difference between $\hat{a}_2$ and a_2. The latter can also be

[1] This setting is based on the solutions of the following equations:

$$
0 \le \frac{1-p}{b_0^2} \le 1; \quad 0 \le 1 - \frac{1-p}{p}\frac{1}{b_0^2} \le 1; \quad 0 \le \frac{(1-p)^2}{pb_0^2} \le 1.
$$

seen in the proposed binomial tree method.

Fig. 6 illustrated the proposed trinomial tree. It is clear that the tree is recombined in all regions, and the jump sizes are different between the high rate regime and the low rate regime. Note that even though different jump sizes exist, their proportional magnitude relation is a constant, equal to $(1-p)/p$. Moreover, unlike the proposed binomial tree, the proxy skew level $\hat{a}_2$ can coincide with the real skew level a_2 in most cases for the trinomial tree, significantly reducing the proxy errors.

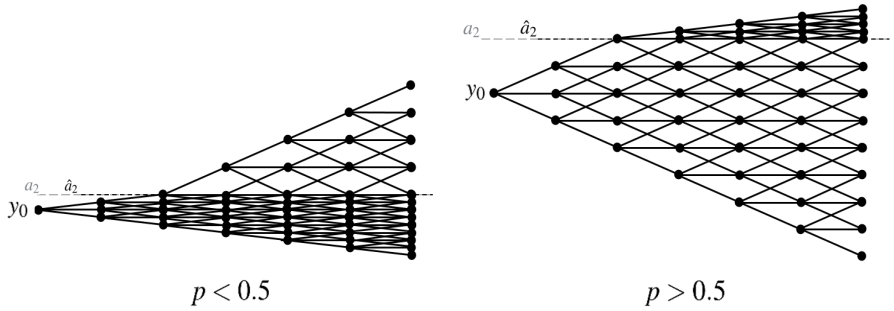

Figure 6: The proposed trinomial tree. When $p < 0.5$, the left panel shows a general piecewise trinomial tree structure in which larger jump-size nodes are located in the high rate regime and smaller jump-size nodes are located in the low rate regime. When $p > 0.5$, the right panel shows a general piecewise trinomial tree structure in which larger jump-size nodes are located in the low rate regime and smaller jump-size nodes are located in the high rate regime.

5. Simulations of Bond and Option Prices

In this section, the prices of zero-coupon bonds and European/American bond options are computed using our proposed piecewise binomial and trinomial lattice approaches. Our model in (1) is general enough to accommodate both the classical Vasicek model and a class of generalized Vasicek models. In fact, the model can be reduced to particular models by giving specific values to some parameters. Our simulations also give us some insights on the patterns of derivative prices in the skew-extended models, and the effects of discontinuity on the drift coefficient.

In Table 1, we compute the prices of zero-coupon bond under the classical Vasicek model using the proposed binomial and trinomial trees, and test the accuracy of these methods by comparing the obtained results with those given by the closed form solutions. We assume the following: the risk-neutral speed k is either 0.1 or 0.5; the initial value of interest rate r_0 is either 5% or 11%; $\theta_1 = \theta_2$ (that is no discontinuity) is either 5%, 8% or 11%; the volatility σ is fixed at 0.1; the bond face value is equal to 100; the maturity of the bond T is either 1 year or 5 year; the bond prices are calculated using $N = 100$ steps and $N = 500$ steps. The skew probability p is set equal to 0.5, so

Table 1: Zero-coupon bond prices under the classical Vasicek model using the proposed binomial and trinomial lattice approach

k	T	r_0	$\theta_1 = \theta_2$	Vasicek	$N = 100$		$N = 500$	
				closed form	binomial	trinomial	binomial	trinomial
0.1	1	0.05	0.05	95.2702	95.2682	95.2682	95.2698	95.2698
0.1	1	0.05	0.08	95.1321	95.1314	95.1314	95.1319	95.1319
0.1	1	0.05	0.11	94.9941	94.9947	94.9947	94.9942	94.9942
0.1	1	0.11	0.05	89.9829	89.9786	89.9786	89.9821	89.9821
0.1	1	0.11	0.08	89.8524	89.8493	89.8493	89.8518	89.8518
0.1	1	0.11	0.11	89.7221	89.7202	89.7202	89.7218	89.7218
0.1	5	0.05	0.05	90.0872	89.9529	89.9673	90.0603	90.0632
0.1	5	0.05	0.08	87.2536	87.1451	87.1574	87.2319	87.2343
0.1	5	0.05	0.11	84.5091	84.4242	84.4352	84.4921	84.4943
0.1	5	0.11	0.05	71.1433	70.9998	71.0162	71.1146	71.1179
0.1	5	0.11	0.08	68.9056	68.7850	68.7982	68.8814	68.8841
0.1	5	0.11	0.11	66.7382	66.6387	66.6494	66.7183	66.7205
0.5	1	0.05	0.05	95.2338	95.2327	95.2328	95.2336	95.2336
0.5	1	0.05	0.08	94.6270	94.6303	94.6303	94.6277	94.6277
0.5	1	0.05	0.11	94.0241	94.0316	94.0317	94.0256	94.0256
0.5	1	0.11	0.05	90.8417	90.8323	90.8325	90.8399	90.8399
0.5	1	0.11	0.08	90.2629	90.2578	90.2579	90.2619	90.2619
0.5	1	0.11	0.11	89.6878	89.6868	89.6869	89.6876	89.6876
0.5	5	0.05	0.05	81.5815	81.5527	81.5859	81.5757	81.5823
0.5	5	0.05	0.08	74.1935	74.1773	74.2090	74.1903	74.1966
0.5	5	0.05	0.11	67.4747	67.4668	67.4992	67.4730	67.4795
0.5	5	0.11	0.05	73.0725	73.0198	73.0540	73.0619	73.0688
0.5	5	0.11	0.08	66.4552	66.4206	66.4485	66.4482	66.4538
0.5	5	0.11	0.11	60.4370	60.4157	60.4403	60.4327	60.4377

Note: $\sigma = 0.1$; $p = 0.5$; $a_1, a_2 \in R$.

that the local time component vanishes and the skew level a_2 can take any value. The continuity of the drift coefficient and the nonexistence of the local time component in our model yield a classical Vasicek model. Table 1 shows that the bond prices obtained by our proposed binomial and trinomial methods are very close to those obtained by their corresponding closed form solutions. This result implies that our approaches are applicable. Moreover, the trinomial lattice performs better than the binomial one, because there are more grids in the trinomial approach, and the trinomial tree can match the drift and volatility perfectly. In addition, the values obtained by both approaches converge to the closed form solutions as the number of steps N increases, and the pricing errors increase as the bond's time to maturity increases.

Table 2 considers the effects of different long-term means and the threshold level, i.e., the influence of the discontinuous drift. In this case, we put $p = 0.5$ such that the local time component is ruled out. The long-term means in different regimes, θ_1 and θ_2 can take the values 5%, 8% or 11%. Since θ_1 belongs to the low interest rate regime and θ_2 belongs to the high one, we intuitively set $\theta_1 < \theta_2$. Meanwhile, the threshold level a_1 can take the values 3%, 6%, 9% and 12%. As a reference, we also list the closed-form solutions for the classical Vasicek model when θ is equal to 5%, 8% and 11%, respectively. It can be seen from Table 2 that bond prices with different long-term means ($\theta_1 \neq \theta_2$) are always between bond prices obtained by the classical Vasicek models for $\theta = \theta_1$ and $\theta = \theta_2$ respectively. For example, in the case of $\theta_1 = 0.05$ and $\theta_2 = 0.08$ (the first row of Table 2), regardless of the values of the threshold level a_1, the bond prices always stay between 95.1321 and 95.2702 which represent the values obtained by the classical Vasicek model when $\theta = 0.08$ and $\theta = 0.05$, respectively. In addition, when the threshold level a_1 becomes larger, the corresponding bond prices also tend to be larger. This is due to the fact that a larger a_1 makes the short rates easily stay in the low interest rate regime, which in turn implies larger bond prices. Furthermore, the speed of convergence is related to the bond's time to maturity, for example, the 1-year bond converges faster than the 5-year bond.

Table 3 explores the influence of the local time. In this situation, $\theta_1 = \theta_2$ so that we can preclude the effects of the discontinuous drift. Since there is no explicit bond solution for the skew Vasicek model, we use prices obtained from the Vasicek closed form solution and prices obtained from the Monte Carlo procedure for reference. The Monte Carlo procedure is based on 100,000 sample paths and 500 discrete points for each path. The prices from our proposed tree methods are quite close to those from the Monte Carlo procedure, which is also a numerical technique. We do not have the explicit bond solutions when $p \neq 0.5$, but our methods apparently outperform the Monte Carlo procedure when $p = 0.5$. Furthermore, it can be seen that when other parameters are fixed, the bond prices are a decreasing function of the skew probability p. In fact, since p is the probability of moving upward when touching the skew level a_2, then larger values of p correspond to larger values of interest rates, that is, smaller values of bond prices. Meanwhile, the bond prices under the skew Vasicek model deviate from those under the classical Vasicek model ($p = 0.5$), and the deviation distance is apparent. This finding provides evidence that the local time indeed exerts non-negligible influence on interest rates. More specifically, the bond deviation distance between skew and non-skew model is correlated with the absolute distance between the skew level a_2 and the initial interest rate r_0. When a_2 is close to r_0, the influence of local time is much stronger and the deviation

Table 2: The influence of different thetas: zero-coupon bond prices under the Vasicek model with discontinuous drift using the proposed binomial and trinomial lattice approaches

T	r_0	θ	Vasicek	θ_1	θ_2	N	$a_1 = 0.03$		$a_1 = 0.06$		$a_1 = 0.09$		$a_1 = 0.12$	
							bin	trin	bin	trin	bin	trin	bin	trin
1	0.05	0.05	95.2702	0.05	0.08	100	95.1717	95.1705	95.2089	95.2142	95.2389	95.2445	95.2545	95.2586
1	0.05	0.05	95.2702	0.05	0.08	500	95.1776	95.1783	95.2176	95.2182	95.2421	95.2451	95.2574	95.2587
1	0.05	0.08	95.1321	0.08	0.11	100	95.0342	95.0330	95.0712	95.0765	95.1014	95.1071	95.1173	95.1215
1	0.05	0.08	95.1321	0.08	0.11	500	95.0390	95.0397	95.0789	95.0795	95.1036	95.1066	95.1191	95.1205
1	0.05	0.11	94.9941	0.05	0.11	100	95.0743	95.0717	95.1488	95.1595	95.2092	95.2206	95.2407	95.2490
1	0.05	0.11	94.9941	0.05	0.11	500	95.0845	95.0858	95.1647	95.1660	95.2141	95.2201	95.2448	95.2475
1	0.11	0.05	89.9829	0.05	0.08	100	89.8585	89.8603	89.8690	89.8752	89.8889	89.8877	89.9241	89.9291
1	0.11	0.05	89.9829	0.05	0.08	500	89.8630	89.8622	89.8737	89.8742	89.8965	89.8972	89.9343	89.9349
1	0.11	0.08	89.8524	0.08	0.11	100	89.7291	89.7309	89.7394	89.7454	89.7590	89.7578	89.7942	89.7991
1	0.11	0.08	89.8524	0.08	0.11	500	89.7326	89.7318	89.7430	89.7436	89.7656	89.7663	89.8033	89.8039
1	0.11	0.11	89.7221	0.05	0.11	100	89.7380	89.7416	89.7587	89.7709	89.7983	89.7959	89.8691	89.8790
1	0.11	0.11	89.7221	0.05	0.11	500	89.7436	89.7419	89.7646	89.7657	89.8101	89.8114	89.8860	89.8872
5	0.05	0.05	90.0872	0.05	0.08	100	88.7903	88.6912	89.0859	89.1993	89.3121	89.5174	89.6125	89.5174
5	0.05	0.05	90.0872	0.05	0.08	500	88.7281	88.7170	89.1087	89.1586	89.4244	89.4973	89.6422	89.7169
5	0.05	0.08	87.2536	0.08	0.11	100	85.9810	85.8831	86.2700	86.3797	86.4931	86.6954	86.7932	86.6954
5	0.05	0.08	87.2536	0.08	0.11	500	85.9028	85.8917	86.2738	86.3223	86.5846	86.6567	86.8018	86.8764
5	0.05	0.11	84.5091	0.05	0.11	100	87.6111	87.3982	88.2057	88.4197	88.6610	89.0601	89.2661	89.0601
5	0.05	0.11	84.5091	0.05	0.11	500	87.3796	87.3545	88.1427	88.2403	88.7781	88.9221	89.2170	89.3646
5	0.11	0.05	71.1433	0.05	0.08	100	69.5859	69.4756	69.7499	69.7410	70.1424	70.0697	70.3709	70.4627
5	0.11	0.05	71.1433	0.05	0.08	500	69.6498	69.6996	69.8681	69.9651	70.1249	70.1172	70.4207	70.4601
5	0.11	0.08	68.9056	0.08	0.11	100	67.3862	67.2784	67.5441	67.5331	67.9255	67.8520	68.1493	68.2367
5	0.11	0.08	68.9056	0.08	0.11	500	67.4339	67.4812	67.6439	67.7372	67.8929	67.8848	68.1818	68.2199
5	0.11	0.11	66.7382	0.05	0.11	100	68.1648	67.9328	68.4885	68.4546	69.2712	69.1088	69.7314	69.8999
5	0.11	0.11	66.7382	0.05	0.11	500	68.1795	68.2742	68.6100	68.7991	69.1211	69.1022	69.7150	69.7912

Note: $\sigma = 0.1$; $k = 0.1$; $p = 0.5$; $a_2 \in R$.

distance is larger than those obtained when a_2 is far from r_0. For example, when $\theta_1 = \theta_2 = 0.05$, the non-skew bond price is 95.2702. In this case, if the skew probability p takes values 0.2 or 0.8, the distance to 95.2702 of the bond prices obtained for $a_2 = 0.06$ (closest to $r_0 = 0.05$) is much larger than that of the bond prices obtained for $a_2 = 0.12$ (farthest to $r_0 = 0.05$). This result is consistent with that of Zhuo *et al.* (2016b), who use a different trinomial tree approach under the skew CIR model, and with that of Zhuo *et al.* (2016a), who use a similar piecewise binomial tree for the skew CEV model. Furthermore, the bond prices decrease as the common long-term means ($\theta_1 = \theta_2$) increase, this is a straightforward consequence of long-term trends in the mean-reverting processes. Notably, the prices calculated by the binomial and trinomial approaches are quite close when the local time does not exist ($p = 0.5$). But when the skew parameter p deviates from 0.5, the difference between the two approaches becomes relatively larger. This occurs partly because the bond price is very sensitive to the skew parameters, resulting in the relatively larger price difference between the two approaches.

Table 4 combines the discontinuous drift coefficient and the local time component, meanwhile the threshold level a_1 and the skew level a_2 have the same value, which could be 3%, 6%, 9% and 12%. In such a setting, the skew probability p controls the probability of entering into the high rate regime, i.e., a higher value of p means there are more opportunities guaranteeing the economy to stay in the high rate state. As a result, the discontinuous drift captures the long-term trends of "good" and "bad" states of the economy, while the local time component describes the speed of entering into one of the states. These two schemes exert a simultaneous influence on the economy. From Table 4, we can observe several "combined" results of Table 2 and Table 3. For instance, the "skew effect" (deviation from non-skew prices) is much stronger when the skew level a_2 is close to the initial short rate r_0. In addition, as a consequence of the "neutralized effect" from different long-term trends, the bond prices in the third panel ($\theta_1 = 0.05, \theta_2 = 0.11$) always stay between their counterparts in the first ($\theta_1 = 0.05, \theta_2 = 0.08$) and second ($\theta_1 = 0.08, \theta_2 = 0.11$) panels. This can be attributed to the discontinuity of the drift coefficient.

Table 5 further generalizes the model and allows for different values of threshold level a_1 and skew level a_2. It can be seen that when the threshold level a_1 is fixed at 0.03 (in the first panel), there exists a non-skew benchmark bond price 95.0858 for the trinomial approach when $N = 500$. As the value of the skew level a_2 becomes closer to the initial short rate $r_0 = 0.05$, the price deviation from 95.0858 becomes larger. Thus when $a_2 = 0.04$, the deviation distance is the largest, with 97.7874 if $p = 0.2$ or 93.1799 if $p = 0.8$. On the other hand, the impact of the local time tends to diminish as

Table 3: The influence of different skew parameters: zero-coupon bond prices under the skew Vasicek model using the proposed binomial and trinomial lattice approaches

$\theta_1 = \theta_2$	a_2	p	Vasicek	$N = 100$		$N = 500$		Monte
			closed form	binomial	trinomial	binomial	trinomial	Carlo
0.05	0.03	0.2	-	97.3063	97.6513	97.0634	97.4947	97.5900
0.05	0.03	0.5	95.2702	95.2682	95.2682	95.2698	95.2698	95.2723
0.05	0.03	0.8	-	93.2556	94.0117	93.1791	93.7042	93.0302
0.05	0.06	0.2	-	97.6762	97.6705	97.7299	97.8839	97.9647
0.05	0.06	0.5	95.2702	95.2682	95.2682	95.2698	95.2698	95.2723
0.05	0.06	0.8	-	92.8604	92.5968	92.9835	93.3768	92.6135
0.05	0.09	0.2	-	96.5465	96.7743	96.5498	96.6657	96.7159
0.05	0.09	0.5	95.2702	95.2682	95.2682	95.2698	95.2698	95.2723
0.05	0.09	0.8	-	93.9741	94.4671	93.9464	94.2183	93.8236
0.05	0.12	0.2	-	95.9064	96.0550	95.8946	95.9724	95.9922
0.05	0.12	0.5	95.2702	95.2682	95.2682	95.2698	95.2698	95.2723
0.05	0.12	0.8	-	94.6155	94.8541	94.5471	94.7428	94.5352
0.08	0.03	0.2	-	97.1619	97.5082	96.9203	97.3552	97.4335
0.08	0.03	0.5	95.1321	95.1314	95.1314	95.1319	95.1319	95.1272
0.08	0.03	0.8	-	93.1512	93.9046	93.0721	93.5981	92.9236
0.08	0.06	0.2	-	97.5528	97.5585	97.6180	97.7683	97.8567
0.08	0.06	0.5	95.1321	95.1314	95.1314	95.1319	95.1319	95.1272
0.08	0.06	0.8	-	92.7415	92.4660	92.8584	93.2610	92.4768
0.08	0.09	0.2	-	96.4280	96.6605	96.4338	96.5519	96.6016
0.08	0.09	0.5	95.1321	95.1314	95.1314	95.1319	95.1319	95.1272
0.08	0.09	0.8	-	93.8342	94.3343	93.8040	94.0814	93.6722
0.08	0.12	0.2	-	95.7845	95.9367	95.7733	95.8530	95.8736
0.08	0.12	0.5	95.1321	95.1314	95.1314	95.1319	95.1319	95.1272
0.08	0.12	0.8	-	94.4706	94.7149	94.3983	94.6001	94.3722
0.11	0.03	0.2	-	97.0172	97.3648	96.7769	97.2155	97.2797
0.11	0.03	0.5	94.9941	94.9947	94.9947	94.9942	94.9942	94.9827
0.11	0.03	0.8	-	93.0469	93.7972	92.9651	93.4919	92.7958
0.11	0.06	0.2	-	97.4291	97.4465	97.5062	97.6527	97.7196
0.11	0.06	0.5	94.9941	94.9947	94.9947	94.9942	94.9942	94.9827
0.11	0.06	0.8	-	92.6230	92.3357	92.7338	93.1454	92.3397
0.11	0.09	0.2	-	96.3097	96.5469	96.3180	96.4384	96.4805
0.11	0.09	0.5	94.9941	94.9947	94.9947	94.9942	94.9942	94.9827
0.11	0.09	0.8	-	93.6947	94.2019	93.6620	93.9449	93.5187
0.11	0.12	0.2	-	95.6629	95.8188	95.6525	95.7340	95.7518
0.11	0.12	0.5	94.9941	94.9947	94.9947	94.9942	94.9942	94.9827
0.11	0.12	0.8	-	94.3260	94.5760	94.2497	94.4577	94.2213

Note: $\sigma = 0.1$; $k = 0.1$; $T = 1$; $r_0 = 0.05$; $a_1 \in R$.

the value of the skew level a_2 moves away from r_0. As for the influence of the discontinuous drift, *ceteris paribus*, the bond price increases as the value of the threshold level a_1 increases, which is consistent with the finding in Table 2.

We consider the patterns of European and American put option prices from Table 6 to Table 10. Table 6 explores the performance of our proposed binomial and trinomial lattice approaches under the classical Vasicek model by comparing our tree results with the closed-form solutions. The underlying asset of the put options is the one-year bond with face value of 100. The maturity of the option, t varies between 0.25 and 0.5 years, and the strike price K can take values 95, 100 and 105. Table 6 shows that the European put prices which are calculated by both the binomial and the trinomial approaches converge rapidly to the closed-form put option prices, and these results hold for a variety of parameter combinations. In addition, American put prices are larger than the corresponding European put prices. Furthermore, the prices computed by these two proposed approaches are quite close for both European and American options. This indicates the effectiveness and consistency of our piecewise binomial and trinomial lattices.

Table 7 examines the influence of different parameter sets of the discontinuous drift $(\theta_1, \theta_2, a_1)$ on the European and American put options. The binomial and trinomial prices are very close, and the differences between the two approaches are in general a bit larger for the American options, compared to those for the European ones. Meanwhile, the price interval restriction is similar to that of Table 2, i.e., the option prices with parameters θ_1 and θ_2 $(\theta_1 \neq \theta_2)$ lie between those under classical Vasicek model with parameters θ_1 and θ_2, respectively. Furthermore, if we fix the values for θ_1 and θ_2, the put option prices decrease when a_1 increases. This pattern is contrary to that of Table 2.

Table 8 investigates the impacts of the local time component and assumes the continuity of the drift coefficient by setting $\theta_1 = \theta_2$. As indicated earlier, we can observe analogous "skew effect", i.e., the option prices are far away from the non-skew benchmark option prices if the skew level a_2 is close to the initial short rate r_0. Table 9 and Table 10 give the impacts of the discontinuous drift coefficient and the local time component, with and without the restriction of $a_1 = a_2$, respectively. In these two tables, both influences of two schemes can be reflected in the option prices, including the price interval restriction stemming from the discontinuous drift, as well as the deviation effect due to the local time.

Table 4: Zero-coupon bond prices under the skew Vasicek model with discontinuous drift using the proposed binomial and trinomial lattice approaches

θ_1	θ_2	$a_1 = a_2$	p	$N = 100$		$N = 500$		Monte
				binomial	trinomial	binomial	trinomial	Carlo
0.05	0.08	0.03	0.2	97.2100	97.5582	96.9688	97.4066	97.4832
0.05	0.08	0.03	0.5	95.1717	95.1705	95.1776	95.1783	95.1722
0.05	0.08	0.03	0.8	93.1713	93.9138	93.0954	93.6123	92.9444
0.05	0.08	0.06	0.2	97.6326	97.6417	97.7027	97.8514	97.9360
0.05	0.08	0.06	0.5	95.2089	95.2142	95.2176	95.2182	95.2104
0.05	0.08	0.06	0.8	92.8010	92.5364	92.9252	93.3118	92.5344
0.05	0.08	0.09	0.2	96.5247	96.7554	96.5325	96.6496	96.6948
0.05	0.08	0.09	0.5	95.2389	95.2445	95.2421	95.2451	95.2376
0.05	0.08	0.09	0.8	93.9448	94.4318	93.9170	94.1866	93.7883
0.05	0.08	0.12	0.2	95.8962	96.0455	95.8868	95.9650	95.9836
0.05	0.08	0.12	0.5	95.2545	95.2586	95.2574	95.2587	95.2519
0.05	0.08	0.12	0.8	94.6019	94.8379	94.5337	94.7280	94.5083
0.08	0.11	0.03	0.2	97.0646	97.4141	96.8246	97.2661	97.3726
0.08	0.11	0.03	0.5	95.0342	95.0330	95.0390	95.0397	95.0614
0.08	0.11	0.03	0.8	93.0665	93.8061	92.9878	93.5056	92.8568
0.08	0.11	0.06	0.2	97.5081	97.5290	97.5901	97.7350	97.8321
0.08	0.11	0.06	0.5	95.0712	95.0765	95.0789	95.0795	95.0987
0.08	0.11	0.06	0.8	92.6815	92.4050	92.7995	93.1953	92.4482
0.08	0.11	0.09	0.2	96.4056	96.6411	96.4159	96.5354	96.6020
0.08	0.11	0.09	0.5	95.1014	95.1071	95.1036	95.1066	95.1258
0.08	0.11	0.09	0.8	93.8043	94.2984	93.7740	94.0490	93.6744
0.08	0.11	0.12	0.2	95.7739	95.9269	95.7653	95.8452	95.8859
0.08	0.11	0.12	0.5	95.1173	95.1215	95.1191	95.1205	95.1404
0.08	0.11	0.12	0.8	94.4566	94.6982	94.3845	94.5848	94.3906
0.05	0.11	0.03	0.2	97.1125	97.4639	96.8728	97.3173	97.3924
0.05	0.11	0.03	0.5	95.0743	95.0717	95.0845	95.0858	95.0823
0.05	0.11	0.03	0.8	93.0863	93.8151	93.0109	93.5196	92.8686
0.05	0.11	0.06	0.2	97.5881	97.6124	97.6750	97.8183	97.9034
0.05	0.11	0.06	0.5	95.1488	95.1595	95.1647	95.1660	95.1623
0.05	0.11	0.06	0.8	92.7411	92.4756	92.8664	93.2461	92.4886
0.05	0.11	0.09	0.2	96.5026	96.7363	96.5149	96.6333	96.6789
0.05	0.11	0.09	0.5	95.2092	95.2206	95.2141	95.2201	95.2165
0.05	0.11	0.09	0.8	93.9152	94.3963	93.8874	94.1545	93.7612
0.05	0.11	0.12	0.2	95.8858	96.0359	95.8790	95.9573	95.9808
0.05	0.11	0.12	0.5	95.2407	95.2490	95.2448	95.2475	95.2456
0.05	0.11	0.12	0.8	94.5881	94.8215	94.5202	94.7130	94.5114

Note: $\sigma = 0.1$; $k = 0.1$; $T = 1$; $r_0 = 0.05$.

Table 5: Zero-coupon bond prices under the generalized skew Vasicek model with discontinuous drift using the proposed binomial and trinomial lattice approaches

a_1	a_2	p	$N = 100$		$N = 500$		Monte
			binomial	trinomial	binomial	trinomial	Carlo
0.03	0.01	0.2	96.4378	96.6637	96.4929	96.5713	96.6905
0.03	0.01	0.5	95.0743	95.0717	95.0845	95.0858	95.1242
0.03	0.01	0.8	93.7464	94.2742	93.7411	94.0184	93.6063
0.03	0.04	0.2	97.5488	96.4374	97.4312	97.7874	97.9275
0.03	0.04	0.5	95.0743	95.0717	95.0845	95.0858	95.1242
0.03	0.04	0.8	92.6643	93.3031	92.6137	93.1799	92.4360
0.03	0.09	0.2	96.3907	96.6213	96.4091	96.5217	96.6093
0.03	0.09	0.5	95.0743	95.0717	95.0845	95.0858	95.1242
0.03	0.09	0.8	93.7723	94.2663	93.7507	94.0308	93.6699
0.03	0.15	0.2	95.3918	95.4523	95.4156	95.4308	95.4906
0.03	0.15	0.5	95.0743	95.0717	95.0845	95.0858	95.1242
0.03	0.15	0.8	94.7533	94.8782	94.7961	94.8320	94.7606
0.08	0.01	0.2	96.5686	96.8249	96.6214	96.7065	96.7867
0.08	0.01	0.5	95.1931	95.1955	95.2006	95.1975	95.2007
0.08	0.01	0.8	93.8444	94.3873	93.8385	94.1143	93.6842
0.08	0.06	0.2	97.6395	97.6310	97.6967	97.8426	97.9360
0.08	0.06	0.5	95.1931	95.1955	95.2006	95.1975	95.2007
0.08	0.06	0.8	92.7667	92.4756	92.9017	93.3011	92.4998
0.08	0.09	0.2	96.4909	96.7363	96.5055	96.6219	96.6797
0.08	0.09	0.5	95.1931	95.1955	95.2006	95.1975	95.2007
0.08	0.09	0.8	93.9007	94.3963	93.8761	94.1456	93.7580
0.08	0.15	0.2	95.5038	95.5809	95.5244	95.5486	95.5618
0.08	0.15	0.5	95.1931	95.1955	95.2006	95.1975	95.2007
0.08	0.15	0.8	94.8789	95.0203	94.9185	94.9555	94.8381
0.13	0.01	0.2	96.6223	96.8675	96.6703	96.7613	96.8368
0.13	0.01	0.5	95.2472	95.2490	95.2501	95.2518	95.2613
0.13	0.01	0.8	93.8985	94.4268	93.8884	94.1627	93.7444
0.13	0.09	0.2	96.5372	96.7606	96.5411	96.6550	96.7189
0.13	0.09	0.5	95.2472	95.2490	95.2501	95.2518	95.2613
0.13	0.09	0.8	93.9444	94.4475	93.9183	94.1951	93.8027
0.13	0.12	0.2	95.8961	96.0438	95.8862	95.9603	96.0011
0.13	0.12	0.5	95.2472	95.2490	95.2501	95.2518	95.2613
0.13	0.12	0.8	94.5908	94.8391	94.5214	94.7247	94.5223
0.13	0.15	0.2	95.5509	95.6165	95.5670	95.5865	95.6150
0.13	0.15	0.5	95.2472	95.2490	95.2501	95.2518	95.2613
0.13	0.15	0.8	94.9392	95.0636	94.9725	95.0083	94.9112

Note: $\theta_1 = 0.05$; $\theta_2 = 0.11$; $\sigma = 0.1$; $k = 0.1$; $T = 1$; $r_0 = 0.05$.

Table 6: European and American put option prices under the classical Vasicek model using the proposed binomial and trinomial lattice approaches

k	t	K	Vasicek closed	European				American			
				$N = 100$		$N = 500$		$N = 100$		$N = 500$	
				bin	trin	bin	trin	bin	trin	bin	trin
0.01	0.25	95	0.8013	0.7999	0.8016	0.8018	0.8008	1.0964	1.0975	1.0987	1.0983
0.01	0.25	100	3.8153	3.8138	3.8164	3.8149	3.8155	4.7623	4.7613	4.7637	4.7632
0.01	0.25	105	8.4459	8.4462	8.4464	8.4460	8.4460	9.7344	9.7344	9.7339	9.7339
0.01	0.5	95	0.4077	0.4088	0.4086	0.4081	0.4078	1.2048	1.2068	1.2090	1.2088
0.01	0.5	100	2.7887	2.7916	2.7876	2.7887	2.7885	4.8257	4.8258	4.8274	4.8271
0.01	0.5	105	7.1839	7.1845	7.1844	7.1840	7.1840	9.7349	9.7349	9.7340	9.7340
0.1	0.25	95	0.7870	0.7866	0.7870	0.7873	0.7869	1.0957	1.0937	1.0962	1.0955
0.1	0.25	100	3.8826	3.8828	3.8811	3.8829	3.8829	4.8790	4.8715	4.8793	4.8791
0.1	0.25	105	8.5658	8.5656	8.5661	8.5658	8.5659	9.8681	9.8681	9.8680	9.8680
0.1	0.5	95	0.3867	0.3877	0.3882	0.3872	0.3869	1.1974	1.1963	1.2006	1.2009
0.1	0.5	100	2.8184	2.8209	2.8192	2.8185	2.8188	4.9231	4.9196	4.9255	4.9243
0.1	0.5	105	7.2751	7.2754	7.2757	7.2751	7.2753	9.8683	9.8683	9.8680	9.8680
0.5	0.25	95	0.7331	0.7358	0.7319	0.7334	0.7336	1.1054	1.1050	1.1051	1.1052
0.5	0.25	100	4.1845	4.1851	4.1851	4.1846	4.1845	5.3722	5.3721	5.3728	5.3728
0.5	0.25	105	9.0252	9.0248	9.0248	9.0252	9.0252	10.3722	10.3721	10.3728	10.3728
0.5	0.5	95	0.3038	0.3031	0.3065	0.3040	0.3041	1.1801	1.1836	1.1832	1.1833
0.5	0.5	100	2.9607	2.9618	2.9609	2.9612	2.9606	5.3714	5.3713	5.3726	5.3726
0.5	0.5	105	7.6236	7.6231	7.6232	7.6235	7.6235	10.3714	10.3713	10.3726	10.3726

Note: $\theta_1 = \theta_2 = 8\%$; $\sigma = 0.1$; $T = 1$; $r_0 = 0.05$; $p = 0.5$; $a_1, a_2 \in R$.

Table 7: The influence of different thetas: European and American put option prices under the Vasicek model with discontinuous drift using the proposed binomial and trinomial lattice approaches

r_0	K	θ	Vasicek closed	θ_1	θ_2	$a_1 = 0.03$				$a_1 = 0.06$			
						European		American		European		American	
						bin	trin	bin	trin	bin	trin	bin	trin
0.05	95	0.05	0.3657	0.05	0.08	0.3866	0.3861	1.1950	1.1949	0.3836	0.3835	1.1818	1.1834
0.05	95	0.08	0.3867	0.08	0.11	0.4084	0.4082	1.2567	1.2568	0.4053	0.4055	1.2429	1.2450
0.05	95	0.11	0.4087	0.05	0.11	0.4077	0.4075	1.2509	1.2507	0.4015	0.4021	1.2237	1.2271
0.05	100	0.05	2.7412	0.05	0.08	2.8014	2.8012	4.8894	4.8877	2.7794	2.7820	4.8510	4.8542
0.05	100	0.08	2.8184	0.08	0.11	2.8798	2.8793	5.0172	5.0146	2.8576	2.8600	4.9787	4.9809
0.05	100	0.11	2.8964	0.05	0.11	2.8627	2.8617	4.9812	4.9782	2.8184	2.8230	4.9040	4.9107
0.11	95	0.05	1.2165	0.05	0.08	1.2643	1.2648	5.1373	5.1369	1.2633	1.2640	5.1246	5.1263
0.11	95	0.08	1.2649	0.08	0.11	1.3144	1.3145	5.2678	5.2675	1.3133	1.3138	5.2554	5.2570
0.11	95	0.11	1.3145	0.05	0.11	1.3141	1.3144	5.2575	5.2568	1.3120	1.3127	5.2325	5.2358
0.11	100	0.05	4.8393	0.05	0.08	4.9231	4.9228	10.1373	10.1369	4.9139	4.9150	10.1246	10.1263
0.11	100	0.08	4.9287	0.08	0.11	5.0127	5.0125	10.2678	10.2675	5.0036	5.0049	10.2554	10.2570
0.11	100	0.11	5.0183	0.05	0.11	5.0070	5.0065	10.2575	10.2568	4.9888	4.9911	10.2325	10.2358
						$a_1 = 0.09$				$a_1 = 0.12$			
0.05	95	0.05	0.3657	0.05	0.08	0.3797	0.3790	1.1654	1.1645	0.3746	0.3745	1.1520	1.1527
0.05	95	0.08	0.3867	0.08	0.11	0.4012	0.4008	1.2260	1.2255	0.3959	0.3961	1.2123	1.2134
0.05	95	0.11	0.4087	0.05	0.11	0.3935	0.3927	1.1905	1.1887	0.3831	0.3835	1.1634	1.1650
0.05	100	0.05	2.7412	0.05	0.08	2.7627	2.7625	4.8253	4.8240	2.7514	2.7527	4.8104	4.8111
0.05	100	0.08	2.8184	0.08	0.11	2.8407	2.8403	4.9529	4.9506	2.8292	2.8303	4.9378	4.9375
0.05	100	0.11	2.8964	0.05	0.11	2.7846	2.7837	4.8523	4.8501	2.7619	2.7639	4.8225	4.8240
0.11	95	0.05	1.2165	0.05	0.08	1.2596	1.2596	5.1035	5.1022	1.2473	1.2486	5.0654	5.0687
0.11	95	0.08	1.2649	0.08	0.11	1.3093	1.3093	5.2345	5.2332	1.2964	1.2982	5.1965	5.1998
0.11	95	0.11	1.3145	0.05	0.11	1.3040	1.3038	5.1904	5.1878	1.2785	1.2815	5.1140	5.1205
0.11	100	0.05	4.8393	0.05	0.08	4.8993	4.8985	10.1035	10.1022	4.8755	4.8775	10.0654	10.0687
0.11	100	0.08	4.9287	0.08	0.11	4.9892	4.9884	10.2345	10.2332	4.9654	4.9675	10.1965	10.1998
0.11	100	0.11	5.0183	0.05	0.11	4.9598	4.9581	10.1904	10.1878	4.9118	4.9159	10.1140	10.1205

Note: $\sigma = 0.1$; $k = 0.1$; $T = 1$; $t = 0.5$; $N = 500$; $p = 0.5$; $a_2 \in R$.

Table 8: The influence of different skew parameters: European and American put option prices under the skew Vasicek model using the proposed binomial and trinomial lattice approaches

$\theta_1 = \theta_2$	a_2	p	Vasicek closed	Monte Carlo	European				American			
					$N = 100$		$N = 500$		$N = 100$		$N = 500$	
					bin	trin	bin	trin	bin	trin	bin	trin
0.05	0.03	0.2	-	1.7001	1.6907	1.7092	1.6970	1.6884	3.0446	3.0034	3.1152	3.0507
0.05	0.03	0.5	2.7412	2.7196	2.7442	2.7416	2.7410	2.7416	4.7954	4.7952	4.7985	4.7983
0.05	0.03	0.8	-	3.8831	3.8330	3.3188	3.8722	3.6326	6.7263	5.9920	6.7901	6.4286
0.05	0.06	0.2	-	1.3149	1.3074	1.3052	1.3282	1.2851	2.2961	2.2739	2.3645	2.2313
0.05	0.06	0.5	2.7412	2.7196	2.7442	2.7416	2.7410	2.7416	4.7954	4.7952	4.7985	4.7983
0.05	0.06	0.8	-	4.2127	3.9570	3.9805	4.1298	3.8537	6.8500	6.9325	7.1532	6.6899
0.05	0.09	0.2	-	1.7488	1.8511	1.7101	1.8342	1.7836	3.5621	3.2499	3.5376	3.4382
0.05	0.09	0.5	2.7412	2.7196	2.7442	2.7416	2.7410	2.7416	4.7954	4.7952	4.7985	4.7983
0.05	0.09	0.8	-	3.7253	3.7904	3.4273	3.7302	3.5564	6.2733	5.7163	6.1861	5.9122
0.05	0.12	0.2	-	2.1481	2.2317	2.1480	2.2217	2.1974	4.1623	4.0220	4.1539	4.1165
0.05	0.12	0.5	2.7412	2.7196	2.7442	2.7416	2.7410	2.7416	4.7954	4.7952	4.7985	4.7983
0.05	0.12	0.8	-	3.3076	3.2973	3.1205	3.2601	3.1991	5.4821	5.2401	5.4386	5.3534
0.08	0.03	0.2	-	1.7449	1.7509	1.7679	1.7628	1.7491	3.1442	3.1062	3.2261	3.1516
0.08	0.03	0.5	2.8184	2.7754	2.8209	2.8192	2.8185	2.8188	4.9231	4.9196	4.9255	4.9243
0.08	0.03	0.8	-	3.9364	3.9055	3.3908	3.9409	3.7017	6.8396	6.0996	6.8973	6.5346
0.08	0.06	0.2	-	1.3530	1.3583	1.3575	1.3795	1.3365	2.3874	2.3689	2.4622	2.3218
0.08	0.06	0.5	2.8184	2.7754	2.8209	2.8192	2.8185	2.8188	4.9231	4.9196	4.9255	4.9243
0.08	0.06	0.8	-	4.2589	4.0408	4.0527	4.2045	3.9240	6.9798	7.0398	7.2674	6.7942
0.08	0.09	0.2	-	1.7862	1.9107	1.7671	1.8921	1.8406	3.6688	3.3506	3.6416	3.5400
0.08	0.09	0.5	2.8184	2.7754	2.8209	2.8192	2.8185	2.8188	4.9231	4.9196	4.9255	4.9243
0.08	0.09	0.8	-	3.7795	3.8732	3.5025	3.8126	3.6348	6.4099	5.8371	6.3196	6.0383
0.08	0.12	0.2	-	2.1921	2.2951	2.2084	2.2839	2.2592	4.2740	4.1264	4.2625	4.2240
0.08	0.12	0.5	2.8184	2.7754	2.8209	2.8192	2.8185	2.8188	4.9231	4.9196	4.9255	4.9243
0.08	0.12	0.8	-	3.3681	3.3813	3.1996	3.3450	3.2805	5.6192	5.3666	5.5749	5.4847
0.11	0.03	0.2	-	1.8207	1.8122	1.8278	1.8301	1.8109	3.2463	3.2121	3.3389	3.2548
0.11	0.03	0.5	2.8964	2.8649	2.8983	2.8974	2.8968	2.8968	5.0517	5.0446	5.0529	5.0510
0.11	0.03	0.8	-	4.0159	3.9782	3.4632	4.0099	3.7712	6.9525	6.2075	7.0044	6.6407
0.11	0.06	0.2	-	1.4153	1.4102	1.4109	1.4318	1.3890	2.4811	2.4689	2.5635	2.4146
0.11	0.06	0.5	2.8964	2.8649	2.8983	2.8974	2.8968	2.8968	5.0517	5.0446	5.0529	5.0510
0.11	0.06	0.8	-	4.3531	4.1244	4.1252	4.2795	3.9946	7.1089	7.1476	7.3818	6.8989
0.11	0.09	0.2	-	1.8551	1.9712	1.8250	1.9514	1.8984	3.7767	3.4543	3.7461	3.6448
0.11	0.09	0.5	2.8964	2.8649	2.8983	2.8974	2.8968	2.8968	5.0517	5.0446	5.0529	5.0510
0.11	0.09	0.8	-	3.8836	3.9566	3.5782	3.8954	3.7137	6.5469	5.9585	6.4534	6.1651
0.11	0.12	0.2	-	2.2617	2.3592	2.2695	2.3468	2.3222	4.3866	4.2323	4.3714	4.3339
0.11	0.12	0.5	2.8964	2.8649	2.8983	2.8974	2.8968	2.8968	5.0517	5.0446	5.0529	5.0510
0.11	0.12	0.8	-	3.4669	3.4660	3.2793	3.4306	3.3626	5.7572	5.4937	5.7116	5.6170

Note: $\sigma = 0.1$; $k = 0.1$; $T = 1$; $t = 0.5$; $K = 100$; $r_0 = 0.05$; $a_1 \in R$.

Table 9: European and American put option prices under the skew Vasicek model with discontinuous drift using the proposed binomial and trinomial lattice approaches

θ_1	θ_2	$a_1 = a_2$	p	Monte Carlo	European				American			
					$N = 100$		$N = 500$		$N = 100$		$N = 500$	
					bin	trin	bin	trin	bin	trin	bin	trin
0.05	0.08	0.03	0.2	1.7795	1.7412	1.7616	1.7522	1.7396	3.1223	3.0859	3.2009	3.1296
0.05	0.08	0.03	0.5	2.8021	2.8029	2.8009	2.8014	2.8012	4.8833	4.8836	4.8894	4.8877
0.05	0.08	0.03	0.8	3.9675	3.8900	3.3870	3.9303	3.6942	6.8084	6.0903	6.8743	6.5180
0.05	0.08	0.06	0.2	1.3718	1.3274	1.3270	1.3481	1.3078	2.3237	2.3047	2.3919	2.2637
0.05	0.08	0.06	0.5	2.7814	2.7828	2.7834	2.7794	2.7820	4.8480	4.8531	4.8510	4.8542
0.05	0.08	0.06	0.8	4.2744	3.9970	4.0274	4.1731	3.9013	6.9027	6.9962	7.2115	6.7549
0.05	0.08	0.09	0.2	1.7972	1.8654	1.7247	1.8468	1.7958	3.5802	3.2688	3.5534	3.4535
0.05	0.08	0.09	0.5	2.7645	2.7661	2.7616	2.7627	2.7625	4.8223	4.8195	4.8253	4.8240
0.05	0.08	0.09	0.8	3.7637	3.8134	3.4542	3.7537	3.5815	6.3015	5.7497	6.2150	5.9432
0.05	0.08	0.12	0.2	2.1848	2.2394	2.1553	2.2270	2.2035	4.1712	4.0306	4.1600	4.1236
0.05	0.08	0.12	0.5	2.7540	2.7556	2.7529	2.7514	2.7527	4.8085	4.8081	4.8104	4.8111
0.05	0.08	0.12	0.8	3.3347	3.3092	3.1342	3.2719	3.2117	5.4956	5.2560	5.4521	5.3680
0.08	0.11	0.03	0.2	1.8612	1.8024	1.8213	1.8192	1.8012	3.2234	3.1907	3.3134	3.2320
0.08	0.11	0.03	0.5	2.9018	2.8803	2.8792	2.8798	2.8793	5.0121	5.0089	5.0172	5.0146
0.08	0.11	0.03	0.8	4.0495	3.9630	3.4595	3.9995	3.7638	6.9222	6.1985	6.9820	6.6246
0.08	0.11	0.06	0.2	1.4371	1.3789	1.3800	1.4000	1.3598	2.4155	2.4005	2.4903	2.3549
0.08	0.11	0.06	0.5	2.8788	2.8601	2.8616	2.8576	2.8600	4.9765	4.9783	4.9787	4.9809
0.08	0.11	0.06	0.8	4.3753	4.0814	4.1001	4.2484	3.9722	7.0332	7.1041	7.3264	6.8599
0.08	0.11	0.09	0.2	1.8632	1.9255	1.7823	1.9051	1.8532	3.6875	3.3701	3.6579	3.5557
0.08	0.11	0.09	0.5	2.8616	2.8433	2.8396	2.8407	2.8403	4.9506	4.9445	4.9529	4.9506
0.08	0.11	0.09	0.8	3.8687	3.8968	3.5299	3.8366	3.6604	6.4387	5.8711	6.3491	6.0699
0.08	0.11	0.12	0.2	2.2569	2.3031	2.2160	2.2895	2.2656	4.2833	4.1352	4.2689	4.2313
0.08	0.11	0.12	0.5	2.8509	2.8326	2.8308	2.8292	2.8303	4.9365	4.9329	4.9378	4.9375
0.08	0.11	0.12	0.8	3.4416	3.3935	3.2136	3.3571	3.2935	5.6332	5.3828	5.5888	5.4997
0.05	0.11	0.03	0.2	1.8485	1.7926	1.8150	1.8085	1.7917	3.2012	3.1700	3.2882	3.2098
0.05	0.11	0.03	0.5	2.8819	2.8623	2.8610	2.8627	2.8617	4.9721	4.9731	4.9812	4.9782
0.05	0.11	0.03	0.8	4.0365	3.9477	3.4557	3.9890	3.7564	6.8913	6.1894	6.9592	6.6083
0.05	0.11	0.06	0.2	1.4060	1.3477	1.3492	1.3683	1.3309	2.3516	2.3360	2.4197	2.2966
0.05	0.11	0.06	0.5	2.8409	2.8219	2.8257	2.8184	2.8230	4.9013	4.9118	4.9040	4.9107
0.05	0.11	0.06	0.8	4.3349	4.0375	4.0748	4.2169	3.9494	6.9559	7.0604	7.2705	6.8206
0.05	0.11	0.09	0.2	1.8197	1.8800	1.7396	1.8596	1.8082	3.5986	3.2881	3.5695	3.4690
0.05	0.11	0.09	0.5	2.8065	2.7882	2.7818	2.7846	2.7837	4.8496	4.8441	4.8523	4.8501
0.05	0.11	0.09	0.8	3.8149	3.8367	3.4813	3.7775	3.6069	6.3300	5.7833	6.2442	5.9745
0.05	0.11	0.12	0.2	2.2063	2.2471	2.1626	2.2324	2.2097	4.1803	4.0393	4.1662	4.1307
0.05	0.11	0.12	0.5	2.7852	2.7671	2.7643	2.7619	2.7639	4.8217	4.8212	4.8225	4.8240
0.05	0.11	0.12	0.8	3.3721	3.3211	3.1480	3.2837	3.2245	5.5093	5.2719	5.4656	5.3827

Note: $\sigma = 0.1$; $k = 0.1$; $T = 1$; $t = 0.5$; $K = 100$; $r_0 = 0.05$.

Table 10: European and American put option prices under the generalized skew Vasicek model with discontinuous drift using the proposed binomial and trinomial lattice approaches

a_1	a_2	p	Monte Carlo	European				American			
				$N = 100$		$N = 500$		$N = 100$		$N = 500$	
				bin	trin	bin	trin	bin	trin	bin	trin
0.03	0.01	0.2	2.3027	2.3096	2.3302	2.3004	2.3018	3.9159	3.9163	3.9406	3.9480
0.03	0.01	0.5	2.8800	2.8623	2.8610	2.8627	2.8617	4.9721	4.9731	4.9812	4.9782
0.03	0.01	0.8	3.6251	3.5377	3.2485	3.5583	3.4129	6.2111	5.8451	6.2423	6.0512
0.03	0.04	0.2	1.5880	1.6230	1.5449	1.5379	1.5096	2.9532	2.6522	2.7650	2.6922
0.03	0.04	0.5	2.8800	2.8623	2.8610	2.8627	2.8617	4.9721	4.9731	4.9812	4.9782
0.03	0.04	0.8	4.2715	4.2496	3.8690	4.2052	3.8637	7.4431	6.8494	7.3705	6.8210
0.03	0.09	0.2	1.8695	1.9368	1.8013	1.9195	1.8687	3.6974	3.3960	3.6738	3.5744
0.03	0.09	0.5	2.8800	2.8623	2.8610	2.8627	2.8617	4.9721	4.9731	4.9812	4.9782
0.03	0.09	0.8	3.8928	3.9186	3.5479	3.8606	3.6802	6.4665	5.8967	6.3825	6.0975
0.03	0.15	0.2	2.5630	2.5793	2.5489	2.5881	2.5686	4.6474	4.6032	4.6664	4.6388
0.03	0.15	0.5	2.8800	2.8623	2.8610	2.8627	2.8617	4.9721	4.9731	4.9812	4.9782
0.03	0.15	0.8	3.2007	3.1267	3.0598	3.1686	3.1024	5.2730	5.1960	5.3346	5.2508
0.08	0.01	0.2	2.2336	2.2426	2.2528	2.2334	2.2323	3.8027	3.7815	3.8261	3.8295
0.08	0.01	0.5	2.8150	2.7954	2.7939	2.7944	2.7948	4.8598	4.8611	4.8663	4.8658
0.08	0.01	0.8	3.5644	3.4772	3.1833	3.4971	3.3502	6.1132	5.7410	6.1426	5.9501
0.08	0.06	0.2	1.3854	1.3363	1.3306	1.3538	1.3165	2.3334	2.3060	2.3969	2.2726
0.08	0.06	0.5	2.8150	2.7954	2.7939	2.7944	2.7948	4.8598	4.8611	4.8663	4.8658
0.08	0.06	0.8	4.3247	4.0162	4.0441	4.1980	3.9142	6.9234	7.0131	7.2403	6.7656
0.08	0.09	0.2	1.8209	1.8849	1.7396	1.8662	1.8129	3.6057	3.2881	3.5791	3.4759
0.08	0.09	0.5	2.8150	2.7954	2.7939	2.7944	2.7948	4.8598	4.8611	4.8663	4.8658
0.08	0.09	0.8	3.8223	3.8429	3.4813	3.7855	3.6109	6.3392	5.7833	6.2560	5.9804
0.08	0.15	0.2	2.5054	2.5188	2.4813	2.5260	2.5042	4.5426	4.4875	4.5586	4.5271
0.08	0.15	0.5	2.8150	2.7954	2.7939	2.7944	2.7948	4.8598	4.8611	4.8663	4.8658
0.08	0.15	0.8	3.1298	3.0538	2.9873	3.0932	3.0294	5.1538	5.0775	5.2115	5.1313
0.13	0.01	0.2	2.2028	2.2086	2.2223	2.1981	2.1987	3.7562	3.7388	3.7774	3.7829
0.13	0.01	0.5	2.7899	2.7602	2.7583	2.7574	2.7585	4.8133	4.8139	4.8170	4.8174
0.13	0.01	0.8	3.5409	3.4413	3.1544	3.4593	3.3164	6.0665	5.7031	6.0930	5.9057
0.13	0.09	0.2	1.8075	1.8581	1.7220	1.8414	1.7923	3.5699	3.2637	3.5457	3.4481
0.13	0.09	0.5	2.7899	2.7602	2.7583	2.7574	2.7585	4.8133	4.8139	4.8170	4.8174
0.13	0.09	0.8	3.7998	3.8169	3.4464	3.7552	3.5779	6.3036	5.7376	6.2147	5.9363
0.13	0.12	0.2	2.2100	2.2395	2.1583	2.2298	2.2064	4.1709	4.0337	4.1629	4.1266
0.13	0.12	0.5	2.7899	2.7602	2.7583	2.7574	2.7585	4.8133	4.8139	4.8170	4.8174
0.13	0.12	0.8	3.3791	3.3171	3.1359	3.2803	3.2172	5.5043	5.2573	5.4615	5.3737
0.13	0.15	0.2	2.4838	2.4894	2.4568	2.4950	2.4748	4.5029	4.4548	4.5163	4.4868
0.13	0.15	0.5	2.7899	2.7602	2.7583	2.7574	2.7585	4.8133	4.8139	4.8170	4.8174
0.13	0.15	0.8	3.0951	3.0148	2.9500	3.0507	2.9900	5.1027	5.0285	5.1556	5.0793

Note: $\theta_1 = 0.05$; $\theta_2 = 0.11$; $\sigma = 0.1$; $k = 0.1$; $T = 1$; $t = 0.5$; $K = 100$; $r_0 = 0.05$.

6. Conclusion

In this paper, we have proposed efficient piecewise binomial and trinomial tree approaches for the generalized skew Vasicek model with discontinuous drift. In order to obtain a free local time transformed process in the tree construction, we have adopted similar techniques used in Zhuo *et al.* (2016a) and Zhuo *et al.* (2016b), then put forward a piecewise binomial tree structure, which has different jump sizes in two subregions to match different volatilities. To ensure the recombination of the tree at the skew level (the boundary level of two subregions), the proxy skew level was proposed to replace the real skew level, and the jump sizes of nodes at the proxy skew level must be modified. One of the main contributions is the extension of this piecewise tree method to the trinomial case. The numerical simulations have demonstrated that both our proposed binomial and trinomial tree methods are efficient and effective. In addition, the piecewise trinomial tree outperforms the piecewise binomial one. Meanwhile, the simulations have also shown many bond and option price features under the generalized Vasicek model with discontinuous drift. For example, the discontinuity of the drift makes bond or option price with two long-term means, θ_1 and θ_2, always lie between its counterparts which only have one long-term mean, either θ_1 or θ_2. There are also apparent price deviation from non-skew price due to the local time, and this deviation is much stronger if the skew level is close to the initial short rate, which we call a "skew effect". We think that the technique introduced in this paper could be extended to the processes with finite skew levels, or the regime-switching models with different volatilities in different states. In addition, it would also be interesting to see what happens when the drift coefficient is time-dependent. Such study requires results on existence and uniqueness of strong solution of (1) when θ_1 and θ_2 are time dependent. This is the object of future research.

Acknowledgments

The project on which this publication is based has been carried out with funding provided by the Alexander von Humboldt Foundation, under the programme financed by the German Federal Ministry of Education and Research entitled "German Research Chair", No 01DG15010; the European Union's Seventh Framework Programme for research, technological development and demonstration under grant agreement No. 318984-RARE; and the Natural Science Foundation of China (No. 71532001, 11571190).

References

T. Appuhamillage & D. Sheldon (2012) First passage time of skew Brownian motion, *Journal of Applied Probability* **49** (3), 685–696.

M. Barlow, K. Burdzy, H. Kaspi & A. Mandelbaum (2000) Variably skewed Brownian motion, *Electronic Communications in Probability* **5**, 57–66.

N. Beliaeva & S. Nawalkha (2012) Pricng American interest rate options under the jump-extended constant-elasticity-of-variance short rate models, *Journal of Banking & Finance* **36**, 151–163.

P. P. Boyle (1988) A lattice framework for option pricing with two state variables, *Journal of Financial and Quantitative Analysis* **23** (1), 1–12.

R. Cantrell & and C. Cosner (1999) Diffusion models for population dynamics incorporating individual behavior at boundaries: applications to refuge design, *Theoretical Population Biology* **55** (2), 189–207.

T. R. A. Corns & S. E. Satchell (2007) Skew Brownian motion and pricing European options, *The European Journal of Finance* **13** (6), 523–544.

M. Decamps, A. De Schepper & M. Goovaerts (2004) Applications of δ-perturbation to the pricing of derivative securities, *Physica A* **342**, 677–692.

M. Decamps, M. Goovaerts & W. Schoutens (2006a) Asymmetric skew Bessel processes and their applications to finance, *Journal of Computational and Applied Mathematics* **186**, 130–147.

M. Decamps, M. Goovaerts & W. Schoutens (2006b) Self exciting threshold interest rates models, *International Journal of Theoretical and Applied Finance* **9**, 1093–1122.

M. Decamps, A. D. Schepper, M. Goovaerts & W. Schoutens (2005) A note on some new perpetuities, *Scandinavian Actuarial Journal* **2005** (4), 261–270.

H. J. Engelbert & W. Schmidt (1991) Strong Markov continuous local martingales and solutions of one-dimensional stochastic differential equations (part iii), *Mathematische Nachrichten* **151**, 149–197.

A. Gairat & V. Shcherbakov (2016) Density of skew Brownian motion and its functionals with application in finance, *Mathematical Finance*, 1–20, doi: 10.1111/mafi.12120.

J. M. Harrison & L. A. Shepp (1981) On skew Brownian motion, *The Annals of Probability* **9** (2), 309–313.

J. C. Hull & A. D. White (1994) Numerical procedures for implementing term structure models I: Single-factor models, *The Journal of Derivatives* **2** (1), 7–16.

K. Itô & H. P. McKean (1965) *Diffusion Processes and Their Sample Paths.* Springer-Verlag.

B. Kamrad & P. Ritchken (1991) Multinomial approximating models for options with k state variables, *Management Science* **37** (12), 1640–1652.

R. Lang (1995) Effective conductivity and skew Brownian motion, *Journal of Statistical Physics* **80** (1), 125–146.

J.-F. Le Gall (1984) One-dimensional stochastic differential equations involving the local times of the unknown process. In: *Stochastic Analysis and Applications*, 51–82. Springer Berlin Heidelberg.

A. Lejay (2003) Simulating a diffusion on a graph: Application to reservoir engineering, *Monte Carlo Methods and Applications* **9** (3), 241–255.

Y. Ouknine (1990) Skew Brownian motion and derived processes, *Theory of Probability & Its Applications* **35** (1), 163–169.

Y. Ouknine & M. Rutkowski (1995) Local times of functions of continuous semimartingales, *Stochastic Analysis and Applications* **13**, 211–231.

G. A. Pfann, P. C. Schotman & R. Tschernig (1996) Nonlinear interest rate dynamics and implications for the term structure, *Journal of Econometrics* **74** (1), 149–176.

P. E. Protter (2005) *Stochastic Integration and Differential Equations*. Springer-Verlag Berlin Heidelberg.

D. Revuz & M. Yor (1999) *Continuous Martingales and Brownian Motion*. New York: Springer.

D. Rossello (2012) Arbitrage in skew Brownian motion models, *Insurance: Mathematics and Economics* **50** (1), 50–56.

S. Song, S. Wang & Y. Wang (2015) First hitting times for doubly skewed Ornstein–Uhlenbeck processes, *Statistics & Probability Letters* **96**, 212–222.

J. B. Walsh (1978) A diffusion with a discontinuous local time, *Astérisque* **52** (53), 37–45.

S. Wang, S. Song & Y. Wang (2015) Skew Ornstein-Uhlenbeck processes and their financial applications, *Journal of Computational and Applied Mathematics* **273**, 363–382.

G. Xu, S. Song & Y. Wang (2016) The valuation of options on foreign exchange rate in a target zone, *International Journal of Theoretical and Applied Finance* **19** (3), 1650020.

M. Zhang (2000) Calculation of diffusive shock acceleration of charged particles by skew Brownian motion, *The Astrophysical Journal* **541** (1), 428–435.

X. Zhuo, G. Xu, Y. Wang & O. Menoukeu-Pamen (2016a) Piecewise binomial lattices for interest rates with long duration under skew CEV model. Submitted.

X. Zhuo, G. Xu & H. Zhang (2016b) A simple trinomial lattice approach for the skew-extended CIR Models. Submitted.